AMERICAN METEOROLOGICAL SOCIETY

Journal of Physical Oceanography

EARLY ONLINE RELEASE

The DOI for this manuscript is doi: 10.1175/JPO-D-13-047.1

Agulhas leakage predominantly responds to the Southern Hemisphere westerlies

Jonathan V. Durgadoo[1]
GEOMAR Helmholtz Centre for Ocean Research Kiel, Germany

Benjamin R. Loveday
Department of Oceanography, University of Cape Town, South Africa

Chris J.C. Reason
Department of Oceanography, University of Cape Town, South Africa

Pierrick Penven
LMI ICEMASA, LPO, UMR 6523 (CNRS, IFREMER, IRD, UBO), France

Arne Biastoch
GEOMAR Helmholtz Centre for Ocean Research Kiel, Germany

[1] *Corresponding author address*: Jonathan Durgadoo, GEOMAR Helmholtz Centre for Ocean Research Kiel, 24105, Germany.
E-mail: jdurgadoo@gmail.com

Abstract

The Agulhas Current plays a crucial role in the thermohaline circulation through its leakage into the South Atlantic. Under both past and present climates, the trade winds and westerlies could have the ability to modulate the amount of Indian-Atlantic inflow. Compelling arguments have been put forward suggesting that trade winds alone have little impact on the magnitude of Agulhas leakage. Here, employing three ocean models for robust analysis – a global coarse resolution, a regional eddy-permitting and a nested high-resolution eddy-resolving configuration – and systematically altering the position and intensity of the westerly wind belt in a series of sensitivity experiments, it is shown that the westerlies, in particular their intensity, control the leakage. Leakage responds proportionally to the westerlies intensity up to a certain point. Beyond this, through the adjustment of the large-scale circulation, energetic interactions occur between the Agulhas Return Current and the Antarctic Circumpolar Current that result in a state where leakage no longer increases. This adjustment takes place within 1 to 2 decades. Contrary to previous assertions, our results further show that an equatorward (poleward) shift in westerlies increases (decreases) leakage. This occurs due to the redistribution of momentum input by the winds. It is concluded that the reported present-day leakage increase could therefore reflect an unadjusted oceanic response mainly to the strengthening westerlies over the last few decades.

1. Introduction

The climatically relevant component of the Agulhas Current system is arguably its inflow into the South Atlantic (de Ruijter et al. 1999). One of the unique features of this western boundary current system is that it redistributes heat and salt not only poleward but also equatorward in the form of Agulhas leakage (Fig. 1). The equatorward injection of warm salty thermocline waters into the Atlantic forms a major part of the return flow towards the North Atlantic, where, through active air-sea interactions at high latitudes, deep waters are formed (Gordon 1986; Gordon et al. 1992; Cunningham and Marsh 2010). In this way, the Agulhas system is considered to be important for global climate (Beal et al. 2011) and as a result, the variability of Agulhas leakage on all timescales is of particular interest. In the past, some evidence for leakage reduction during glacial times (Peeters et al. 2004), possibly modulated by a northward migration of the subtropical front south of Africa (Bard and Rickaby 2009), has been inferred from sediment records. At glacial terminations, increase in leakage has been further linked with the recovery of the Atlantic thermohaline circulation (Knorr and Lohmann 2003). Under the current (and future) warming climate, model studies suggest an increasing trend in Agulhas leakage (Biastoch et al. 2009a; Rouault et al. 2009) that result in an overall salinification of the South Atlantic (Biastoch and Böning 2013). The effectiveness of this significant exchange south of Africa for the most part is thought to be linked in one way or another to the wind patterns of the Southern Hemisphere (Biastoch et al. 2009a; Rouault et al. 2009).

The Agulhas system is sandwiched between two major wind belts, namely the southeast trades, between the Equator and about 30°S, and the westerlies, over roughly 30° – 60°S. With the average latitudinal range of the positive wind stress curl region in

the Indian Ocean extending beyond the termination of the African continent near 34°S (Marshall and Plumb 2007), the Agulhas Current leaves the continental slope as a free-jet. An interplay between its large inertia and the position of the zero wind stress curl (maximum westerlies) leads to its retroflection (Ou and de Ruijter 1986), a process which also determines the amount of leakage into the Atlantic (de Ruijter et al. 1999; Pichevin et al. 1999; Dijkstra and de Ruijter 2001). Therefore, the variability of Agulhas leakage on all timescales is expected to be connected to the trades and/or westerlies strength and/or position.

The trade winds are largely responsible for the inertia of the Agulhas Current. Rouault et al. (2009) and van Sebille et al. (2009) (who used the same model as Biastoch et al. (2009a)) found the contemporary increase in leakage to be linked with the upstream strength of the Agulhas Current. Within their range of model observations, they however disagreed on the sign of the relationship; Rouault et al. (2009) claimed an increase in leakage caused by increase in Agulhas Current, while van Sebille et al. (2009) argued for a decrease in the upstream inertia that leads to an increase in leakage. Both of these studies implied that the trade winds influence leakage magnitude. In a series of realistic global and regional ocean/sea-ice models, Loveday et al. (submitted) showed that the sensitivity of Agulhas leakage to the Agulhas Current transport decreases with increasing horizontal resolution. In the eddy-resolving simulations, large changes in the upstream transport of the Agulhas Current had almost no effect on the magnitude of the leakage. Even though a stronger Agulhas transport did cause the Agulhas Current to break from the shelf further upstream (Ou and de Ruijter 1986), the inertial jet always proceeded south-westward. As a result, despite large localized changes in both mean and eddy

kinetic energy, the annual mean retroflection position remained stable, consistent with observed present-day (Dencausse et al. 2010) and reconstructed past (Franzese et al. 2009) measurements, and Agulhas leakage is unaffected. The increase in kinetic energy possibly leads to a recently described turbulent retroflection regime (Le Bars et al. 2012) where leakage is no longer dependent on the incoming transport.

Given this apparent decoupling between Agulhas leakage and trade winds, in this study we explore the possible dependency of leakage on the Southern Hemisphere westerlies. We systematically alter the position and magnitude of the westerly wind belt within three model configurations similar to those used by Biastoch et al. (2009a) and van Sebille et al. (2009) (half-degree global, with and without a tenth-degree nest) and Rouault et al. (2009) (quarter-degree regional) in order to achieve robust results. The strategy we employ generally follows the works of Oke and England (2004), Sijp and England (2008, 2009) and Biastoch and Böning (2013). The models are all forced by the same atmospheric data and consistent diagnostics are derived. In so-doing, we aim to dis-entangle the relationship between the magnitude of Agulhas leakage and the westerlies location and strength.

Following a description of the models and of our experiment strategy in section 2 we explore the equilibrium (section 3) and transient (section 4) leakage response to westerlies change. In section 5 we seek a mechanism explaining the results and then discuss the implications in section 6 before summarizing our main findings in section 7.

2. Model configurations and Experiment Strategy

The three models employed in this study are ORCA05, INALT01 and AGIO. The first two, based on the ocean/sea-ice Nucleus for European Modeling of the Ocean code

(NEMO v3.1.1, Madec (2008)) and developed under the DRAKKAR framework (The DRAKKAR Group 2007) are global models and will be described first. AGIO, summarized thereafter, is a regional model based on the Regional Ocean Modeling System (ROMS, Shchepetkin and McWilliams (2005)) and is described thoroughly in Loveday et al. (submitted). Similar configurations of these models were used by Biastoch et al. (2009a), Rouault et al. (2009) and van Sebille et al. (2009) but with different setups and forcing fields which we hypothesize have led to their conflicting results. To assess this, we performed all experiments under same atmospheric forcing with as much coherence and conformity as possible.

a. ORCA05 and INALT01

Both ORCA05 (coarse resolution configuration) and INALT01 (nested configuration) follow an ORCA setup (Madec and Imbard 1996; Barnier et al. 2006). In this setup a tri-polar horizontal grid is used and south of 20°N, the grid is Mercator-type. Variables are staggered following an Arakawa-C arrangement. In the vertical, the model uses z-coordinates with a total of 46 levels (10 levels in the top 100 m and a maximum of 250 m resolution at depth). In order to enhance representation of flow near bottom topography, the deepest grid box is allowed to be partially filled (Barnier et al. 2006) in addition to a non-linear bottom friction (Tréguier 1992). A free-slip lateral momentum boundary condition is used. The treatment of tracers is implemented using a Laplacian operator for the lateral diffusion and the Total Variance Dissipation (Zalesak 1979) scheme for advection. Lateral diffusion on momentum uses a bi-Laplacian operator with a vector form advection scheme that conserves energy and enstrophy (Arakawa and Hsu 1990).

Sub-grid scale vertical mixing is calculated explicitly through the turbulent eddy kinetic dependent diffusion scheme (Blanke and Delecluse 1993).

ORCA05, with half-degree nominal horizontal resolution, which in the Agulhas region is ~45 km, is an established configuration successfully reproducing the large-scale global circulation (Biastoch et al. 2008a). INALT01 consists of a base global model (that is identical in configuration to ORCA05) and a nest embedded within between 70°W – 70°E and 50°S – 8°N (Fig. 1). The nest refines the horizontal model grid over the Agulhas Current system and South Atlantic 5-folds to a tenth-degree (~9 km over the Agulhas region). This also implies a 4-fold time-stepping refinement from 36 (base) to 9 (nest) minutes. Bathymetry within the nest region is interpolated from ETOPO2[1].

The horizontal refinement is achieved by adopting the AGRIF (Debreu and Blayo 2008) approach whereby both model grids are coupled in a 2-way mode at every base model time-step to provide the nest with open boundary conditions from the base but also enabling the mesoscale dynamics of the nest to permeate into the base. For this reason, neither INALT01's base nor ORCA05 have parameterized mesoscale eddies, a practice that is usually common for models of such resolution class. Eddy parameterization, such as the Gent and McWilliams (1990) scheme, typically mimics the impact of eddies on tracer fluxes as isopycnal diffusion and eddy advection. This has an overall effect of reducing isopycnal steepness. Such parameterization is believed to dampen the influence of the mesoscale dynamics of the nest onto the base. ORCA05 was also run without eddy parameterization in order to allow consistent comparison between both models.

INALT01 is an update of AG01 (Biastoch et al. 2009b), the latter has been demonstrated to represent the dynamics of the Agulhas Current and its large-scale impact

[1] http://www.ngdc.noaa.gov/mgg/global/relief/ETOPO2/ETOPO2v2-2006/ETOPO2v2g/

161 successfully (Biastoch et al. 2008b,c, 2009a,b; van Sebille et al. 2009). With its wider
162 high-resolution domain encompassing the South Atlantic basin as well as the tropical
163 Atlantic, INALT01 better lends itself to the investigation of the hypothesized impact of
164 Agulhas leakage on the Atlantic heat, freshwater and momentum balances. In addition,
165 the advective pathways between the Agulhas system and the North Atlantic can be
166 further explored. The new configuration simulates successfully two major western
167 boundary currents of the Southern Hemisphere.

168 Prescribing appropriate atmospheric forcing is crucial for ocean modeling. The
169 CORE (v2b, Large and Yeager (2009)) project provides the necessary coherent and
170 globally balanced dataset to drive the model. Through bulk formulation, 6-hourly air-sea
171 fluxes of heat, freshwater and momentum, daily short- and long-wave radiation and
172 monthly rain and snow, are used in conjunction with surface ocean temperatures and
173 velocities, which effectively allow some feedback between ocean and atmosphere. For
174 this study, both climatologically and inter-annually varying CORE fields were used.

175 Ocean-only models often exhibit drifts in properties. In order to constrict such
176 artificial drifts within ORCA05 and INALT01, a 10 % precipitation reduction (which
177 falls within the CORE dataset uncertainty range) north of 55°N is implemented in
178 addition to a sea surface salinity restoring over the top 50 m with a timescale of 8.3 years.
179 This "very weak" salt flux damping is capped at 0.5 kg m^{-1} s^{-1} to prevent regions of
180 strong gradients from being excessively damped.

181 Initializing the thermohaline fields with a combined dataset from Levitus World
182 Ocean Atlas 1998[1] and Polar Science Centre Hydrographic Climatology (Steele et al.
183 2001), and starting from rest, ORCA05 is allowed to spin-up for 20 years forced with

[1] http://www.esrl.noaa.gov/psd/

184 inter-annually (1978-1997) varying CORE fields. This strategy promotes a stable Atlantic
185 meridional overturning circulation with a reasonable magnitude of ~18 Sv (Cunningham
186 and Marsh 2010) which, in the previous version (AG01), was ~10 Sv (Biastoch et al.
187 2008b). Dynamic equilibrium is reached within the 20 years of spin-up (Fig. 2) and this
188 output is then used to warm-start the experiments outlined in Section 2c.

189 *b. AGIO*

190 The AGIO configuration (Loveday et al. submitted) is a quarter-degree resolution eddy-
191 permitting implementation of ROMS (Shchepetkin and McWilliams 2005), constructed
192 using ROMSTOOLS (Penven et al. 2008). The domain, which extends from 29°W to
193 115°E and 48°S to 7°N on a Mercator grid, spans the Indian and South East Atlantic
194 Ocean basins. AGIO is an extension of the SAfE configuration (Penven et al. 2006)
195 which was used by Rouault et al. (2009). The average grid spacing over the southern
196 Agulhas region is ~23 km. The vertical resolution in AGIO is described by 32 σ-
197 coordinate levels following the GEBCO1[1] derived bathymetry and stretched towards the
198 surface. The regional bathymetry is selectively smoothed to reduce pressure gradient
199 errors (Haidvogel and Beckmann 1999). Higher order numerics and a third-order,
200 upstream-biased advection scheme reduce dispersion, allowing steep density gradients to
201 be preserved, and enhancing precision for a given resolution (Shchepetkin and
202 McWilliams 1998). The splitting of diffusion and advection via the RSUP3 scheme
203 minimizes spurious diapcynal mixing (Marchesiello et al. 2009). Western boundary
204 currents are selectively damped via a parameterization of horizontal viscosity
205 (Smagorinsky 1963) and sub-grid scale vertical mixing follows a non-local K-Profile

[1] http://www.gebco.net/data_and_products/gridded_bathymetry_data/

parameterization (Large et al. 1994). The lateral viscosity and diffusion are zero in the domain interior and increase to 1000 m^2 s^{-1} in the sponge layer within ~200 km from the domain boundaries. Prognostic variables are connected to the external conditions by an active radiation scheme (Marchesiello et al. 2001). Lateral boundary conditions for all AGIO experiments are derived from the climatological-monthly-mean ORCA05 reference experiment, and variability associated with the Antarctic Circumpolar Current is thereby excluded. AGIO is initialized with outputs from the ORCA05 20-year spin-up.

c. Experiment Design and Application

The experiments we performed are to some extent similar to those presented by Oke and England (2004) and Sijp and England (2008, 2009). Anomalies applied to the present-day wind patterns (Fig. 3a) were designed to mimic different states in westerlies regime; equatorward and poleward shifts of ±2° and ±4° of latitude (Fig. 3b) and intensity changes of ±20 % and ±40 % (Fig. 3c). The values chosen roughly span the range of observed (Swart and Fyfe 2012), 21st century projected (Fyfe and Saenko 2006; Fyfe et al. 2007) as well as past (Hodgson and Sime 2010) changes in westerly winds. These anomalies have a smooth and quasi-sinusoidal shape to avoid any sharp changes or disruptions in the general wind stress curl pattern (that would alter the general pattern of the circulation). Additional design considerations were: (*i*) Changes to the westerlies were limited to south of 35°S such that no changes are applied to the latitudes that would influence the inertia of the western boundary current; (*ii*) Shifts were constructed based on the latitudinal location of the maximum wind stress and the total energy input kept constant; (*iii*) The meridional wind stress component were unchanged. These considerations imposed limits to the extent the westerlies could be altered.

229 The resulting anomalies were reproduced onto the respective model-grids. Out of
230 the 8 anomalies (Fig. 3b, c), a total of 15 anomaly fields were produced (Table 1). For
231 some anomalies, in particular the SHW+40% anomaly (westerlies intensity increase by
232 40%), in addition to changing the intensity of the wind stress, we also altered the region
233 over which these anomalies were applied (Fig. 4). These geographical decompositions
234 attempt to determine the influence the Antarctic Circumpolar Current may have on the
235 Agulhas system. For these cases, additional smoothing was applied along the boundaries.
236 The 2-dimensional wind anomaly fields were added after calculation of the wind stress.
237 Thus, the application influences the momentum and not the buoyancy input to the
238 ocean/sea-ice. This strategy follows Biastoch and Böning (2013) who performed a similar
239 experiment within AG01.
240 All three models, sharing the same 20-year spin-up history, were forced under
241 background CORE climatological forcing (Large and Yeager 2009). Fig. 2 exemplifies
242 the adjustment of the models. A relatively fast adjustment in volume integrated kinetic
243 energy to changes in resolution and forcing (application of anomaly) is noted. The
244 reference experiments were integrated for 30 years before application of the anomalies.
245 At first they were applied with a linear ramp-up over one year (model year 31) and
246 subsequently in full. Reference and sensitivity simulations ran parallel from model year
247 31. After two decades of parallel integration, analysis for all simulations was performed
248 for a common period of 10 years (model years 51 – 60). The increasing kinetic energy
249 after model year 45 in the global models for the SHW+40% examples shown in Fig. 2
250 reflects the transient response of the Agulhas system to the enhanced winds. This is
251 discussed in Section 4. Some selected experiments were extended, as outlined in Table 1.

The models were additionally integrated under inter-annually varying surface forcing, providing 6 decades (1948 – 2007) of hind-cast simulations.

d. Model Validations

Given the dominance of mesoscale variability, direct one-to-one comparison with features observed during oceanographic expeditions cannot be expected, even though a high-frequency, inter-annually varying forcing is used. However, time-mean properties and statistical representation of the variability ought to be comparable. ORCA05 is an established configuration of NEMO (Biastoch et al. 2008a). Both AGIO and INALT01 are updates of previously thoroughly tested configurations; SAfE (Penven et al. 2006) and AG01 (Biastoch et al. 2008b,c,2009b; van Sebille et al. 2009,2010) respectively. Within ORCA05, the Agulhas Current is represented by a continuous flow that begins in the Northern Mozambique Channel with the only source of variability originating south of Madagascar. The current retroflects and occasionally produces some large unrealistic rings. In contrast, within AGIO and INALT01, where the first baroclinic Rossby radius of deformation is resolved (20 – 50 km in this region, Chelton et al. (1998)), a broad spectrum of mesoscale activity is observed in the known source regions of the Agulhas Current as well as a more realistic representation of the diverse range of features typically found in the Cape Cauldron, namely Agulhas Rings, Cyclones and filaments among others (Boebel et al. 2003). Fig. 5 portrays the models reproduction of the mean circulation as well as the mesoscale variability of the Agulhas system compared to that observed from satellite altimetry (Fig. 5a). The mean circulation is successfully represented by all three models; the details of the variability do however differ.

e. Assessing Agulhas leakage

Measuring Agulhas leakage is no simple task. Being highly intermittent, leakage occurs predominantly through Agulhas rings. However, other features such as cyclones and filaments also contribute to the Indian-Atlantic transport. Therefore, direct quantification of Agulhas rings crossing the Cape Basin would likely underestimate leakage magnitude (de Ruijter et al. 1999), while full-depth Eulerian measurements would over estimate it. Attempts at estimating leakage using optimized Eulerian methods have been made (van Sebille et al. 2010) but the skills of such methods have not been tested across models with different horizontal and vertical resolutions. From float and drifter observations, Richardson (2007) estimated leakage to be at about 15 Sv.

Here, we estimated annual values of leakage using a Lagrangian method following the works of Speich et al (2001), Biastoch et al. (2008b, 2009a) and van Sebille et al. (2009). Water parcels were released every 5 days for one year over the full-depth of the poleward-flowing Agulhas Current across a zonal 300 km long segment at 32°S. Each parcel had a defined transport of max. 0.1 Sv and the total number of parcels released were representative of the 5-daily magnitude of the Agulhas Current. The parcels were then advected using the model's velocity fields for a total period of five years and aggregated across predefined sections. The integration period optimally allowed 98 % of the parcels to exit the domain shown in Fig. 5d. Agulhas leakage is defined as that portion of the Agulhas Current exiting the domain through the Good-Hope section (Ansorge et al. 2005) in the Cape Basin (Fig. 5b). The advantage of this method is that it can be applied to all three models without the need for additional model-specific redefinitions, allowing direct inter-model comparisons. The southward transport of the

297 Agulhas Current at 32°S for model years 51 – 60 of the three REF experiments are 71.9 ±
298 0.7, 72.9 ± 3.1 and 64.6 ± 2.6 Sv for ORCA05, AGIO and INALT01 respectively. The
299 corresponding reference leakage values for the same period are 31.9 ± 1.5, 31.5 ± 1.4 and
300 16.6 ± 1.7 Sv respectively. It is clear that leakage is markedly influenced by the regional
301 mesoscale (Biastoch et al. 2008c).

302 3. Agulhas leakage equilibrium response

303 Owing to the different reference values of Agulhas leakage in the three models, we adopt
304 the percentage change with respect to reference as a measure of leakage response. This
305 places all reference values at the origin. The 10-year-mean (model years 51 – 60) leakage
306 response to changes in position (Fig. 6a) and intensity (Fig. 6b) of the westerlies display
307 three clear patterns. Firstly, within the global models, an equatorward (poleward) shift in
308 westerlies produces an increase (decrease) in leakage. Note that AGIO's southern
309 boundary at 48°S makes shift experiments not sensible. Secondly, increasing westerlies
310 intensity generally produces more leakage but the relationship is not completely linear.
311 Finally, leakage responds preferentially, and the magnitude of that response is more
312 pronounced when changes are applied to the westerlies intensity than shifts. For this
313 reason, we will concentrate on the intensity cases and return to the shifts towards the end.
314 Interestingly, for strong wind stress in Fig. 6b, both global models simulate very little
315 leakage change and even reduction compared to the reference values. Conversely, a 20 %
316 and 40 % reduction in wind stress produces approximately the same amount of leakage
317 decrease. Consistent with Le Bars et al. (2012), there appears to be a threshold in leakage
318 response to increased westerlies.

In order to investigate the reason for this threshold, we focus on two extreme intensity cases, SHW±40% within ORCA05. The Agulhas system, forming part of the subtropical gyres of the south Atlantic and south Indian Oceans (Ridgway and Dunn 2007) and bounded by the Antarctic Circumpolar Current, potentially could be influenced by numerous external factors. In an attempt to therefore distinguish between local and large-scale wind impact on leakage, a geographical decomposition of the SHW±40% experiments was performed (Fig. 4a-c). We favored the use of the coarse resolution ORCA05 model since it is computationally less demanding. The response shown in Fig. 6c reveals that the overall leakage response consists of the direct influence of the westerlies acting locally (over the Agulhas Retroflection and Cape Basin region) on the magnitude of the leakage and on the indirect influence of the winds via the adjacent currents. INALT01, the configuration that mimics the known complexity of the Agulhas system with the highest degree of semblance, reproduces the general behavior in leakage. Leakage response within INALT01-SHW+40% with LOCAL decomposition shows that, despite the overestimation of absolute leakage values within the coarse resolution model, the change in leakage is consistent. The decompositions further indicate that the threshold in leakage change originates from the large-scale circulation, within which the Agulhas system is embedded.

This hypothesis is tested by employing the regional model, AGIO, whose domain excludes much of the large-scale circulation (Loveday et al. submitted). The global ocean influences this regional model through lateral boundary conditions derived from climatology of the ORCA05-REF simulation. Here, leakage response is quasi-linear, monotonously increasing with strengthening westerlies (Fig. 6b). This suggests that, with

a constant climatological representation of large-scale circulation, in particular that of the Southern Ocean, the portion of the westerlies felt within AGIO's southern domain (35°S – 48°S) does not cause a threshold in leakage response. Altering the boundary conditions to that derived from the ORCA05-SHW+40% experiment (red cross in Fig. 6b), effectively allows for an assessment of the influence a different Southern Ocean state have on leakage. In this case, leakage behavior is similar to that of the two global models, supporting the hypothesis that the threshold observed in leakage (Fig. 6b) originates from the large-scale circulation.

4. Agulhas leakage transient response to increased westerlies

For the purpose of exploring the time dependency of Agulhas leakage response to increased westerlies, we focus on the SHW+40% case and expand the ORCA05 simulations to beyond the 10 years of common analysis. Fig. 7 shows the time evolution of leakage and other parameters associated with the greater Agulhas system. Presented, are the annual values beginning from model year 31, which is when the anomaly fields are applied. Linear trends calculated from the reference experiment were removed from all runs. Under background climatological forcing, these minor trends (between 0.1 % and 2.5 % of the reference values per decade) represent the inherent numerical drift that can reasonably be assumed to be similar in all simulations. The BASIN and LOCAL decompositions are overlaid. Following a fast initial adjustment, three distinct stages in leakage behavior in the ORCA05-SHW+40%-FULL case (red curve on Fig. 7) can be noted; (*i*) A proportional increase (model year 34 – 47) followed by (*ii*) a rapid decline

364 (model year 47 – 50) and finally (*iii*) return to and decadal modulation around reference
365 values (beyond model year 50).

366 Stage-1: Lasting for about a decade, during Stage-1, the westerlies acting both
367 locally and outside the Agulhas region contribute towards increasing the leakage. This
368 produces an overall proportional response (40 % increase in winds resulting in ~40 %
369 increase in leakage), with a 1:3 ratio between LOCAL and BASIN. During Stage-1, the
370 mean value of leakage for the FULL experiment is significantly different at the 99 %
371 confidence level (Welch's t-test) from the mean leakage value of the reference
372 experiment. As anticipated, no change is observed in the Agulhas Current, the Agulhas
373 Return Current (ARC) and Mozambique throughflow, since surface forcing is unchanged
374 equatorward of 35°S. The Antarctic Circumpolar Current (ACC) and south-west Indian
375 sub-gyre, during that period, adjust to the altered forcing, which thereafter determines the
376 timescale of the leakage response. Note that, we opt to measure the barotropic ACC
377 transport south of the African continent, the region that is most likely to impact the
378 Agulhas system. Qualitatively, there is little difference from measuring at other choke
379 points, at Drake Passage for example, where the reference value of ACC transport is
380 about 130 Sv, falling within observed ranges (Meredith et al. 2011).

381 Stage-2: Happening rapidly, within 4 model years (47 – 50), the decline appears
382 to occur indirectly as a result of the large-scale circulation adjustment. Without the large-
383 scale adjustment, a local increase in westerlies would maintain an increased leakage. The
384 decline coincides with the peak in ACC, the increase in ARC transport and variability,
385 and owing to the subtropical gyre spin-up, the increase in Mozambique throughflow. The
386 Agulhas Current also begins to respond accordingly.

Stage-3: Approximately 2 decades after the initial anomaly application, leakage falls within the variability range of the reference experiment (with some decadal variations around it). For Stage-3, the mean leakage value of the FULL experiment is significantly not different at 99 % confidence level from the reference value. In response to a 40 % increase in westerlies, the ACC stabilizes to ~20 % above reference (Fig. 7). The strengthened sub-gyre results in the increase in Mozambique Channel flow (by ~25 %) and subsequent downstream increase of the Agulhas Current (by ~5 %). This Agulhas Current transport increase occurs as an indirect effect of the westerlies increase. No change in the East Madagascar Current transport is noted (not shown). The ARC speed remains at an increased level (~23 % above reference values), with a ~60 % increase in variance. Towards the end of the simulation (model year 90 onwards), due the increased wind stress curl acting only over the southern portion of the subtropical gyres, the stronger sub-gyre meridionally contracts and zonally widens. This is subsequently seen in a slight reduction in Mozambique throughflow and Agulhas Current transport. The return of leakage to reference values occurs due to the large-scale circulation, as suggested by the BASIN experiment.

Fig. 8 shows the equivalent within INALT01. Comparing the two global models provides a way of diagnosing the impact mesoscale activities of the wider Agulhas region have on the leakage response. Perhaps surprisingly so, but as already seen in Fig. 6, the general response to westerly winds increase is not altered. The adjustment happens quicker, and Stage-3 is reached 2 – 3 years earlier. To test the impact of resolution on domain decomposition, the LOCAL experiment (only decomposition falling entirely within INALT01's nest boundaries) was repeated within INALT01. The response is as

anticipated similar (Figs. 6b and 8). The fact that the models agree in the response, irrespective of resolution, points towards an underlying mechanism that is to some extent resolution independent.

The response seems to be linked to the development of the ACC. In the Atlantic sector of the Southern Ocean, an increase in westerlies promotes a spin-up of the Weddell gyre and, due to an increased pressure gradient, also its expansion (not shown). This in turn, leads to an overall increase in the width of the circumpolar current in the Atlantic. Within the two global models, the dynamic front between the supergyre and the ACC regime can be diagnosed from the zero barotropic stream-function line (see Fig. 3a). During Stage-3, immediately south of the leakage corridor, this boundary migrates by ~2° equatorward.

In the Southern Ocean, resolving eddies is known to be important (Hallberg and Gnanadesikan 2006; Böning et al. 2008; Spence et al. 2010). The ACC within INALT01 is represented at the same resolution as within ORCA05. Owing to the 2-way nesting scheme adopted for INALT01 and the requirement for consistent comparisons across models, the choice has been made not to parameterize eddies in ORCA05. However in order to assess the dependence of the 3-stage response on firstly Southern Ocean eddies and secondly on initial conditions, we repeated the ORCA05-REF and ORCA05-SHW+40%-FULL experiments including the initial 20-year spin-up with parameterized eddies (Gent and McWilliams 1990). Thickness diffusivities used are capped at 1000 m^2 s^{-1} but vary spatially and temporally, increasing with stratification and isopycnal slope. These simulations showed the same 3-stage behavior in leakage response (including the

magnitude of the Stage-1 increase), with the only difference being a prolonged Stage-2 (figure not shown).

Seeking to confirm that the ACC generally influences Agulhas leakage, three additional experiments were undertaken. In these experiments, the SHW+40% anomaly field was further decomposed geographically and applied within ORCA05 (Fig. 4d-f). Fig. 9 shows the general behavior in ACC-B and ACC-L following the same 3-stage pattern as for FULL (Fig. 7). Within the given time frame, no response is seen when the ACC-P decomposition is applied, potentially indicating that the westerlies acting over the Pacific Ocean, Drake Passage and south of Australia, under this set-up, have no direct immediate impact on leakage. A possible reason for this would be that the westerlies, generally weaker in strength and lying about 5° poleward in the Pacific compared to the Indian-Atlantic sector (Fig. 3), are not aligned to the core of the applied anomaly. The response in ACC-B, similar in magnitude to that of FULL, suggests that the winds in the region 18°W – 115°E, corresponding to the region of maximum climatological westerlies (Fig. 3), sets the leakage response. Further confirming the ACC's influence, ACC-L, a poleward extension of the LOCAL application, shows an initial increase of the same magnitude as LOCAL and a subsequent 3-stage leakage response.

The time scale is set by the ACC. Following the ACC peak, both the leakage and ARC (transport and variance) react with a decline and increase respectively (Figs. 7 – 9). Averaging over two 5-year periods reveals that in Stage-1, the leakage increase is coincidental with an increased eddy kinetic energy in the Cape Basin but a decrease in the retroflection region (Fig. 10a,c). Flowing adjoined and unidirectional to each other, the interaction between the ACC and the ARC become important in Stage-3, where both

455 the retroflection and the ARC become more energetic and variable (Figs. 7 – 9, 10b,d).
456 This is characteristic of a turbulent retroflection regime (Le Bars et al. 2012). This
457 regime, which occurs at strong winds, leads to the increased volume transport (seen in
458 Stage-1 as increased leakage) to be lost through an enhanced interaction between the
459 ARC and the ACC.

460 5. Mechanism of leakage response to the westerlies

461 The region of positive wind stress curl in the South Indian and South Atlantic oceans
462 roughly lies between 15ºS (maximum trades) and 50ºS (maximum westerlies). The wind
463 stress curl yields negative Ekman vertical velocities (i.e. pumping) over this region,
464 which promotes an equatorward Sverdrup transport of the interior (Marshall and Plumb
465 2007). Fig. 11 schematically portrays the proposed mechanism of leakage response to
466 changes in the westerlies. Increasing the westerlies in the manner presented in this study
467 leads to an increased wind stress curl between the latitudes 35° and 50ºS. The
468 equatorward interior flow across the southern portion of the supergyre is therefore
469 enhanced. In Fig. 11, this is depicted along 40°S, which roughly is the latitude of
470 separation between the westward flowing Agulhas leakage and the eastward flowing
471 Agulhas Return Current. By construction no change is applied to the winds at the
472 latitudes of the Agulhas Current, north of 35°S. Through continuity, the increased
473 meridional transport must result in a westward mass transport towards the South
474 America. Closing the circulation, the western boundary current subsequently increases.
475 Figs. 6b and 6c (gray lines) also show the change in theoretical meridional interior
476 flow (Sverdrup transport) along 40°S resulting from the added intensity anomalies. As
477 anticipated, the change in Sverdrup transport is a linear function of the change in wind

stress curl. Our results show that leakage change within the global models follows the proportional Sverdrup transport change over the entire time-series for the reduced westerlies cases (Fig 6b) and during Stage-1 of the intensified westerlies simulations (Figs 7 and 8).

In the portrayal shown in Fig. 11, leakage corresponds to the westward flow south of the African continent and is a passive component of the supergyre circulation. This has three major implications. Firstly, it suggests that the process determining leakage would be independent of retroflection energetics. In partial support for this, we showed that eddy kinetic energy of the retroflection in Fig. 10 matches in sign with neither the initial increase in leakage of Stage-1 nor the return to reference values in Stage-3. Eddy kinetic energy of the retroflection is increased in Stage-3 compared to reference levels, while leakage is unchanged. Therefore, there seems to be no link between the energetics of the retroflection and the process behind leakage. Secondly, it backs up the conclusion of Loveday et al. (submitted) who showed leakage to be decoupled from changes in the Agulhas Current. During Stage-1, large response in leakage occurs without any change in Agulhas Current. In Stage-3, the increase in Agulhas Current (an indirect consequence of the westerlies increase) results in no change in leakage. Thirdly, as noted in Figs. 6 – 8, the general pattern of leakage response to the westerlies change is reflected at all resolutions; in other words, irrespective of the form of leakage. It is important to mention here that we do not claim that leakage follows Sverdrup dynamics since non-linearity plays a crucial role in determining the amount of water entering the South Atlantic. What we noticed is that, given a change in the westerlies, leakage responds in the same way the interior adjustment (described by the Sverdrup balanced) does.

Agulhas leakage response is transient (Figs 7 – 9). The time dependency is a question of wave propagation, in particular internal planetary waves, similar to the process that communicates the dynamical imprint of leakage across the South Atlantic (van Sebille and van Leeuwen 2007, Biastoch et al. 2008b). Rossby waves set the adjustment time of the ocean to large-scale forcing. The initial rapid oceanic adjustment to the applied high-frequency wind forcing prior to Stage-1 (model years 31 – 33) is a result of the fast propagation of barotropic Rossby waves, which establishes the Sverdrup balance. Meanwhile, the westerly winds influence induces a baroclinic adjustment of the eastward flowing ACC on decadal timescale. Additional controls, such as its width, its variability and buoyant convection within and outside of the current further influence the adjustment timescale of the ACC (Allison et al. 2011). The timing in Figs. 7 – 9 suggests that the interaction between the ACC and the Agulhas system become important after 1 – 2 decades. The decrease in leakage in Stage-3 is preceded by an increasing variability of the ARC, which occurs when the ACC reaches its peak. The precise mechanism behind this interaction is beyond the scope of this study. Since both currents are unidirectional and adjacent, meridional exchanges in lateral momentum and tracers between them may be a likely explanation.

Thus far, we focused on the impact of westerlies intensity on the Agulhas system. As noted earlier, idealized equatorward shifts of the westerly wind belt induces an increase in leakage (Fig. 6a). This occurs as a result of the redistribution of momentum. Our application of a northward shift of the westerlies strengthens the wind stress curl between 35° and 45°S, while reducing it over the core of ACC (45° – 60°S). The overall effect is similar to an increase in westerlies over the southern portion of the Indian Ocean

subtropical gyre which leads to an increase in leakage. In this case, leakage remains at a constant increased level (persistent Stage-1) and a weaker ACC does not result in leakage to be hampered. The opposite for poleward shifts also holds; reduced northward Sverdrup transport across the southern boundary of the supergyre boundary leads to reduced leakage. Towards the end of the SHW-4 simulation, there is an indication that the leakage further decreases, exacerbated by an increased ACC which stimulates an enhanced interaction with the retroflection and ARC. This, once again, is dynamically consistent as described above.

6. Discussion

There is the common belief that a displacement of the zero wind stress curl line equatorward (poleward) would narrow (widen) the gateway south of Africa allowing less (more) leakage (Zahn, 2010). Our result shows the converse. Paleoceanographic interpretations propose that, on centennial-millennial timescales, a displacement of the subtropical front at the northern boundary of the ACC south of Africa, concomitant with shifts and intensity changes in the westerlies, could be a major driver in modulating the amount of leakage (Peeters et al. 2004; Bard and Rickaby 2009; Caley et al. 2012). In our series of experiments, we observed no significant change in the latitudinal position of the hydrographically-defined subtropical front (maximum temperature gradient) south of Africa in response to changes in position of the zero wind stress curl line. However, we cannot emphatically conclude that the front does not respond to westerly changes, since we did not apply a corresponding thermohaline forcing. Our ocean/sea-ice only simulations addressed the transient response of the Agulhas system. Processes such as deep and bottom water formation, which indirectly respond to changing wind patterns,

547 would in the long term affect the hydrography of the Southern Ocean leading to possible
548 shifts of its fronts (Spence et al. 2010; Downes et al. 2011; Graham et al. 2012).
549 During the Last Glacial Maximum (~20 kyears ago), leakage reduction (Peeters et
550 al. 2004; Franzese et al. 2006), and possible ACC increase (Franzese et al. 2006; Otto-
551 Bliesner et al. 2006) with no change in retroflection position (Franzese et al. 2009) have
552 been suggested. There is, however, large uncertainty regarding the state of the Southern
553 Hemisphere winds during glacial times (Kohfeld et al. 2013). To name but a few
554 examples of recent studies, Anderson et al. (2002) and Wyrwoll et al. (2000) reported an
555 intensifying poleward displacement of the westerly jet; Rojas et al. (2008) concluded a
556 decrease with no significant latitudinal shift while Toggweiler et al. (2006) deduced an
557 equatorward shift. It is therefore not possible, given the present limited knowledge of the
558 wind patterns of the Last Glacial Maximum, to confirm whether or not the dependency of
559 Agulhas leakage on the westerlies was dominant. Nonetheless, a leakage reduction
560 accompanied by a more vigorous ACC would be in line with our results.
561 Of current relevance, models simulate an increase in contemporary Agulhas
562 leakage (Biastoch et al. 2009b; Rouault et al. 2009). Biastoch et al (2009b) proposed that
563 a poleward shift in contemporary westerlies is responsible for this increase. Swart et al.
564 (2012) questioned the robustness of such a latitudinal shift in present-day westerlies in an
565 analysis of various coupled climate model products as well as observational reanalyzes
566 and found that instead significant strengthening of the westerlies rather than shift has
567 occurred. In the last 40 years, the westerlies have increased by about 25 % (Fig. 12). We
568 showed that leakage initially responds proportionally to increased westerlies (Stage-1 in
569 Figs. 7 and 8). In Fig. 12, this is reflected by the linear relationship for the SHW+20%

570 and SHW+40% cases. Note that Fig. 12 shows the area-averaged (20°W – 140°E, 35° –
571 65°S) change in westerlies and not the change in maximum zonal-averaged westerlies.
572 Also shown are decadal averages in leakage change derived from the hind-cast
573 experiments of ORCA05 and INALT01. Given the strong linear relationship (r = 0.98
574 and 0.96 for ORCA05 and INALT01 respectively), similar to that of the sensitivity
575 experiments, we can conclude that the upward trend in leakage reported by Biastoch et al.
576 (2009b) and Rouault et al. (2009) may reflect an unadjusted oceanic response to the
577 continuously increasing momentum input by the westerlies akin to Stage-1. We could
578 further speculate that, should the on-going wind change lessen or halt (Watson et al.
579 2012) in response to stratospheric ozone recovery (Son et al. 2010), future decadal trend
580 in leakage could weaken. This would naturally also depend on the timing and magnitude
581 of the ACC response. It is unclear whether or not the ACC is already eddy saturated
582 (Hallberg and Gnanadesikan 2006; Böning et al. 2008; Spence et al. 2010). We have
583 shown that the circumpolar current plays a relatively critical role in the transient 3-stage
584 leakage response. Therefore, should the ACC be weakly responsive (or unresponsive) to
585 the present-day increasing westerlies, a delay in the onset of a Stage-2-type leakage
586 response can be expected.

587 Rouault et al. (2009) and van Sebille et al. (2009) both related the strength of the
588 Agulhas Current with the magnitude of leakage. Within the present-day range of
589 transport values, they found a linear relationship between the two variables. They did,
590 however, disagree on the sign of that relationship. Results presented here suggest that
591 changes in leakage do not necessitate variations in upstream transport. The Agulhas
592 Current is influenced by both easterlies (Loveday et al. submitted) and westerlies (this

593 study, Stage-3), while leakage responds predominantly to the westerlies. The
594 disagreement between Rouault et al. (2009) and van Sebille et al. (2009) was most likely
595 an outcome of the different wind field products used in forcing their respective models.
596 In general, within an integral large-scale atmospheric system, statistical relationships
597 between the Agulhas Current and leakage do not necessarily imply cause and impact but
598 instead are manifestations of individual external forcing.

599 Resolution is an important aspect of Agulhas system modeling. The necessity to
600 resolve the Agulhas system adequately has been amply emphasized in the literature (e.g.
601 Biastoch and Krauss 1999; Biastoch et al. 2008c). Beal et al. (2011) even recommend
602 that at least a tenth degree horizontal resolution (e.g. INALT01) is required. Such
603 resolution has not yet been reached by most coupled climate models used for future
604 predictions (Taylor et al. 2012; Weijer et al. 2012). Here, while our series of experiments
605 demonstrate that leakage response to a constant change in westerly winds is represented
606 at all resolutions, we wish to stress the importance in considering the magnitude of the
607 response. For example, a 40 % increase in westerlies during Stage-1 results in
608 approximately the same percentage increase in leakage, which at low-resolution
609 (ORCA05) is ~10 Sv and at high-resolution (INALT01) is ~6 Sv. Coarse resolution
610 models clearly overestimate the actual volumetric transport and corresponding amount of
611 heat and salt exported into the Atlantic, which ultimately is of critical importance because
612 of the implications for the Atlantic meridional overturning circulation and global climate
613 (Biastoch et al. 2008b,c). Notwithstanding, within the 0.5° – 0.1° range, the mechanism
614 behind the response of leakage to changes in the westerlies is consistent.

Our study describes leakage response in the context of changes in the zonal component of westerlies that are constant in time. In reality, the wind system changes progressively and leakage is expected to respond non-linearly to the compounding effects of migrations and magnitudes (deviation from linearity seen in Fig. 12). The meridional component of the wind stress, albeit relatively small on average, may additionally play a role which we have not considered here. Furthermore, changes in the transition zone between the easterlies and westerlies (between 25° and 35°S) as well as the impact of altered wind forcing on the thermohaline field may also be important.

7. Summary

We systematically deconstructed the manner in which the Southern Hemisphere westerlies affect Agulhas leakage and reached the conclusion that the intensity of the wind belt is predominantly responsible in controlling the Indian-Atlantic transport. Agulhas leakage responds rapidly (within 2 – 3 years) and proportionally to changes in the westerly wind stress. Change in leakage is comparable to the change in Sverdrup transport across the southern portion of the supergyre. Shifts and modifications to the intensity of the wind belt result in changes in wind energy input that, following Sverdrup dynamics, cause an adjustment of the interior flow. South of Africa, that change is in turn reflected as a change of leakage.

Simulations where the intensity of the westerlies was increased show a transient response in leakage. Initially, leakage responds proportionally to the wind increase. Subsequently, after 1 – 2 decades, leakage subsides to normal reference levels. The transient response occurs due to the adjustment of the large-scale circulation. In

637 particular, energetic interactions between the Antarctic Circumpolar Current and the
638 Agulhas system cause the subsidence in leakage.

639 We also showed that the impact a displacement of the westerly wind belt has on
640 leakage can be regarded as a redistribution of momentum. Shifts of the westerlies
641 equatorward increase the energy input over the southern portion of the supergyre and
642 reduce it over the Southern Ocean. This results in enhanced leakage. Conversely,
643 poleward shifts reduces leakage and the reduction would be accentuated following the
644 adjustment (strengthening) of the circumpolar current. This result is at odds with previous
645 claims.

646 Our investigation further suggested that the process behind the leakage response
647 to changes in the westerlies is independent of model resolution, upstream transport of the
648 Agulhas Current and possibly retroflection energetics. However, this does not discredit
649 the importance of non-linearity in the region. The volumetric change in leakage within
650 models is highly dependent on the correct representation of the numerous non-linear
651 interactions in the Agulhas system. More importantly, the corresponding changes in the
652 amount of heat and salt being exported have the potential of impacting the circulation in
653 the Atlantic.

654

655 *Acknowledgments.*

656 This work received funding from the European Community's Seventh Framework
657 Programme FP7/2007-2013-Marie-Curie ITN, under grant agreement 238512,
658 GATEWAYS project. Model experiments were performed at the High performance
659 computing centres in Stuttgart (HLRS) and in Cape Town (CHPC) as well as at the

Christian-Albrechts University of Kiel (NESH). The Ariane-v2.2.6 Lagrangian package was used for Agulhas leakage calculation (http://www.univ-brest.fr/lpo/ariane/). Altimetry data for model validation were downloaded from http://aviso.oceanobs.com.

References

Allison, L. C., H. L. Johnson, and D. P. Marshall, 2011: Spin-up and adjustment of the Antarctic Circumpolar Current and global pycnocline. *J. Mar. Res.*, **69**, 167–189, doi:10.1357/002224011798765330.

Anderson, R. F., Z. Chase, M. Q. Fleisher, and J. Sachs, 2002: The Southern Ocean's biological pump during the Last Glacial Maximum. *Deep-Sea Res. II*, **49**, 1909–1938, doi:10.1016/S0967-0645(02)00018-8.

Ansorge, I., S. Speich, J. R. E. Lutjeharms, G. J. Goni, C. J. de W. Rautenbach, P. Froneman, M. Rouault, and S. L. Garzoli, 2005: Monitoring the oceanic flow between Africa and Antarctica: Report of the first GoodHope cruise. *S. Afr. J. Sci.*, **101**, 29–35.

Arakawa, A., and Y.-J. G. Hsu, 1990: Energy conserving and potential-enstrophy dissipating schemes for the shallow water equations. *Mon. Wea. Rev.*, **118**, 1960–1969.

Bard, E., and R. E. M. Rickaby, 2009: Migration of the subtropical front as a modulator of glacial climate. *Nature*, **460**, 380–383, doi:10.1038/nature08189.

Barnier, B. and Coauthors, 2006: Impact of partial steps and momentum advection schemes in a global ocean circulation model at eddy-permitting resolution. *Ocean Dyn.*, **56**, 543–567, doi:10.1007/s10236-006-0082-1.

683 Beal, L. M., W. P. M. de Ruijter, A. Biastoch, R. Zahn, and SCOR/WCRP/IAPSO-
684 Working-Group-136, 2011: On the role of the Agulhas system in ocean
685 circulation and climate. *Nature*, **472**, 429–436, doi:10.1038/nature09983.
686 Biastoch, A., and W. Krauss, 1999: The Role of Mesoscale Eddies in the Source Regions
687 of the Agulhas Current. *J. Phys. Oceanogr.*, **29**, 2303–2317.
688 Biastoch, A., C. W. Böning, J. Getzlaff, J.-M. Molines, and G. Madec, 2008a: Causes of
689 Interannual–Decadal Variability in the Meridional Overturning Circulation of the
690 Midlatitude North Atlantic Ocean. *J. Climate*, **21**, 6599–6615,
691 doi:10.1175/2008JCLI2404.1.
692 Biastoch, A., C. W. Böning, and J. R. E. Lutjeharms, 2008b: Agulhas leakage dynamics
693 affects decadal variability in Atlantic overturning circulation. *Nature*, **456**, 489–
694 492, doi:10.1038/nature07426.
695 Biastoch, A., J. R. E. Lutjeharms, C. W. Böning, and M. Scheinert, 2008c: Mesoscale
696 perturbations control inter-ocean exchange south of Africa. *Geophys. Res. Lett.*,
697 **35**, L20602, doi:10.1029/2008GL035132.
698 Biastoch, A., C. W. Böning, F. U. Schwarzkopf, and J. R. E. Lutjeharms, 2009a: Increase
699 in Agulhas leakage due to poleward shift of Southern Hemisphere westerlies.
700 *Nature*, **462**, 495–498, doi:10.1038/nature08519.
701 Biastoch, A., L. M. Beal, J. R. E. Lutjeharms, and T. G. D. Casal, 2009b: Variability and
702 Coherence of the Agulhas Undercurrent in a High-Resolution Ocean General
703 Circulation Model. *J. Phys. Oceanogr.*, **39**, 2417–2435,
704 doi:10.1175/2009JPO4184.1.

705 Biastoch, A., and C. W. Böning, 2013: Anthropogenic Impact on Agulhas Leakage.
706 *Geophys. Res. Lett.*, **40**, 1–6, doi:10.1002/grl.50243.
707 Blanke, B., and P. Delecluse, 1993: Variability of the tropical Atlantic Ocean simulated
708 by a general circulation model with two different mixed-layer physics. *J. Phys.*
709 *Oceanogr.*, **23**, 1363–1388.
710 Boebel, O., J. Lutjeharms, C. Schmid, W. Zenk, T. Rossby, and C. Barron, 2003: The
711 Cape Cauldron: a regime of turbulent inter-ocean exchange. *Deep-Sea Res. II*, **50**,
712 57–86.
713 Böning, C. W., A. Dispert, M. Visbeck, S. R. Rintoul, and F. U. Schwarzkopf, 2008: The
714 response of the Antarctic Circumpolar Current to recent climate change. *Nature*
715 *Geosci.*, **1**, 864–869, doi:10.1038/ngeo362.
716 Caley, T., J. Giraudeau, B. Malaizé, L. Rossignol, and C. Pierre, 2012: Agulhas leakage
717 as a key process in the modes of Quaternary climate changes. *P. Natl. Acad. Sci.*
718 *USA*, **109**, 6835–6839, doi:10.1073/pnas.1115545109.
719 Chelton, D. B., R. A. DeSzoeke, M. G. Schlax, E. N. Karim, and S. Nicolas, 1998:
720 Geographical variability of the first baroclinic Rossby radius of deformation. *J.*
721 *Phys. Oceanogr.*, **28**, 433 – 460.
722 Cunningham, S. A., and R. Marsh, 2010: Observing and modeling changes in the Atlantic
723 MOC. *Wiley Interdisciplinary Reviews: Climate Change*, **1**, 180–191,
724 doi:10.1002/wcc.22.
725 de Ruijter, W. P. M., A. Biastoch, S. S. Drijfhout, J. R. E. Lutjeharms, R. P. Matano, T.
726 Pichevin, P. J. van Leeuwen, and W. Weijer, 1999: Indian-Atlantic interocean

727 Dynamics , estimation and impact ring shedding. *J. Geophys. Res.*, **104**, 20885 –
728 20910.
729 Debreu, L., and E. Blayo, 2008: Two-way embedding algorithms: a review. *Ocean Dyn.*,
730 **58**, 415–428, doi:10.1007/s10236-008-0150-9.
731 Dencausse, G., M. Arhan, and S. Speich, 2010: Spatio-temporal characteristics of the
732 Agulhas Current retroflection. *Deep-Sea Res. I*, **57**, 1392–1405,
733 doi:10.1016/j.dsr.2010.07.004.
734 Dijkstra, H. A., and W. P. M. de Ruijter, 2001: On the Physics of the Agulhas Current:
735 Steady Retroflection Regimes. *J. Phys. Oceanogr.*, **31**, 2971–2985.
736 Downes, S. M., a. S. Budnick, J. L. Sarmiento, and R. Farneti, 2011: Impacts of wind
737 stress on the Antarctic Circumpolar Current fronts and associated subduction.
738 *Geophys. Res. Lett.*, **38**, 3–8, doi:10.1029/2011GL047668.
739 Franzese, A., S. Hemming, S. Goldstein, and R. Anderson, 2006: Reduced Agulhas
740 Leakage during the Last Glacial Maximum inferred from an integrated
741 provenance and flux study. *Earth Planet. Sci. Lett.*, **250**, 72–88,
742 doi:10.1016/j.epsl.2006.07.002.
743 Franzese, A. M., S. R. Hemming, and S. L. Goldstein, 2009: Use of strontium isotopes in
744 detrital sediments to constrain the glacial position of the Agulhas Retroflection.
745 *Paleoceanography*, **24**, PA2217, doi:10.1029/2008PA001706.
746 Fyfe, J. C., and O. A. Saenko, 2006: Simulated changes in the extratropical Southern
747 Hemisphere winds and currents. *Geophys. Res. Lett.*, **33**, L06701,
748 doi:10.1029/2005GL025332.

749 Fyfe, J. C., O. A. Saenko, K. Zickfeld, M. Eby, and A. J. Weaver, 2007: The Role of
750 Poleward-Intensifying Winds on Southern Ocean Warming. *J. Climate*, **20**, 5391–
751 5400, doi:10.1175/2007JCLI1764.1.
752 Gent, P. R., and J. C. McWilliams, 1990: Isopycnal Mixing in Ocean Circulation Models.
753 *J. Phys. Oceanogr.*, **20**, 150–155.
754 Gordon, A. L., 1986: Interocean exchange of Thermocline Water. *J. Geophys. Res.*, **91**,
755 5037–5046, doi:10.1029/JC091iC04p05037.
756 Gordon, A. L., R. F. Weiss, W. M. Smethie, and M. J. Warner, 1992: Thermocline and
757 Intermediate Water Communication between the South Atlantic and Indian
758 Oceans. *J. Geophys. Res.*, **97**, 7223–7240.
759 Graham, R. M., A. M. de Boer, K. J. Heywood, M. R. Chapman, and D. P. Stevens,
760 2012: Southern Ocean fronts: Controlled by wind or topography? *J. Geophys.*
761 *Res.*, **117**, 1–14, doi:10.1029/2012JC007887.
762 Haidvogel, D. B., and A. Beckmann, 1999: *Numerical Ocean Circulation Modeling*.
763 Series on Environmental Science and Management: Volume 2, 344pp.
764 Hallberg, R., and A. Gnanadesikan, 2006: The Role of Eddies in Determining the
765 Structure and Response of the Wind-Driven Southern Hemisphere Overturning:
766 Results from the Modeling Eddies in the Southern Ocean (MESO) Project. *J.*
767 *Phys. Oceanogr.*, **36**, 2232–2252, doi:10.1175/JPO2980.1.
768 Hodgson, D. a., and L. C. Sime, 2010: Palaeoclimate: Southern westerlies and CO2.
769 *Nature Geosci.*, **3**, 666–667, doi:10.1038/ngeo970.

770 Knorr, G., and G. Lohmann, 2003: Southern Ocean origin for the resumption of Atlantic
771 thermohaline circulation during deglaciation. *Nature*, **424**, 532–536,
772 doi:10.1038/nature01855.
773 Kohfeld, K.E., R. M. Graham, A. M. de Boer, L. C. Sime, E. W. Wolff, C. Le Quéré, and
774 L. Bopp, 2013: Southern Hemisphere westerly wind changes during the Last
775 Glacial Maximum: paleo-data synthesis. *Quat. Sci. Rev,*, **68**, 76–95,
776 doi:10.1016/j.quascirev.2013.01.017.
777 Large, W. G., J. C. Mcwilliams, and S. C. Doney, 1994: Oceanic vertical mixing: A
778 review and a model with a nonlocal boundary layer parameterization. *Rev.*
779 *Geophys.*, **32**, 363–403.
780 Large, W. G., and S. G. Yeager, 2009: The global climatology of an interannually
781 varying air–sea flux data set. *Climate Dyn.*, **33**, 341–364, doi:10.1007/s00382-
782 008-0441-3.
783 Le Bars, D., W. P. M. de Ruijter, and H. A. Dijkstra, 2012: A New Regime of the
784 Agulhas Current Retroflection: Turbulent Choking of Indian–Atlantic leakage. *J.*
785 *Phys. Oceanogr.*, **42**, 1158–1172, doi:10.1175/JPO-D-11-0119.1.
786 Loveday, B. R., J. V. Durgadoo, C. J. C. Reason, A. Biastoch, and P. Penven, Decoupling
787 of the Agulhas Current from the Agulhas Leakage. *J. Phys. Oceanogr.*, submitted.
788 Madec, G., 2008: *NEMO ocean engine*. Note du Pole de modeisation de l'Institut Pierre-
789 Simon Laplace No 27, **ISSN No 12**, 215pp.
790 Madec, G., and M. Imbard, 1996: A global ocean mesh to overcome the North Pole
791 singularity. *Climate Dyn.*, **12**, 381–388, doi:10.1007/BF00211684.

792 Marchesiello, P., J. C. McWilliams, and A. Shchepetkin, 2001: Open boundary
793 conditions for long-term integration of regional oceanic models. *Ocean Modell.*,
794 **3**, 1–20, doi:10.1016/S1463-5003(00)00013-5.
795 Marchesiello, P., L. Debreu, and X. Couvelard, 2009: Spurious diapycnal mixing in
796 terrain-following coordinate models: The problem and a solution. *Ocean Modell.*,
797 **26**, 156–169, doi:10.1016/j.ocemod.2008.09.004.
798 Marshall, J., and R. Plumb, 2007: *Atmosphere, ocean and climate dynamics: an*
799 *introductory text*. Academic Press, 334pp.
800 Meredith, M. P. and Coauthors, 2011: Sustained monitoring of the Southern Ocean at
801 Drake Passage: Past achievements and future priorities. *Rev. Geophys.*, **49**,
802 RG4005, doi:10.1029/2010RG000348.
803 Oke, P., and M. England, 2004: Oceanic response to changes in the latitude of the
804 Southern Hemisphere subpolar westerly winds. *J. Climate*, **17**, 1040–1054.
805 Otto-Bliesner, B. L., E. C. Brady, G. Clauzet, R. Tomas, S. Levis, and Z. Kothavala,
806 2006: Last Glacial Maximum and Holocene Climate in CCSM3. *J. Climate*, **19**,
807 2526–2544, doi:10.1175/JCLI3748.1.
808 Ou, H., and W. de Ruijter, 1986: Separation of an inertial boundary current from a curved
809 coastline. *J. Phys. Oceanogr.*, **16**, 280–289.
810 Peeters, F. J. C., R. Acheson, G.-J. a Brummer, W. P. M. de Ruijter, R. R. Schneider, G.
811 M. Ganssen, E. Ufkes, and D. Kroon, 2004: Vigorous exchange between the
812 Indian and Atlantic oceans at the end of the past five glacial periods. *Nature*, **430**,
813 661–665, doi:10.1038/nature02785.

814 Penven, P., J. R. E. Lutjeharms, and P. Florenchie, 2006: Madagascar: A pacemaker for
815 the Agulhas Current system? *Geophys. Res. Lett.*, **33**, L17609,
816 doi:10.1029/2006GL026854.
817 Penven, P., P. Marchesiello, L. Debreu, and J. Lefèvre, 2008: Software tools for pre- and
818 post-processing of oceanic regional simulations. *Environ. Modell. Softw.*, **23**,
819 660–662, doi:10.1016/j.envsoft.2007.07.004.
820 Pichevin, T., D. Nof, and J. R. E. Lutjeharms, 1999: Why are there Agulhas Rings. *J.*
821 *Phys. Oceanogr.*, **29**, 693–707.
822 Richardson, P. L., 2007: Agulhas leakage into the Atlantic estimated with subsurface
823 floats and surface drifters. *Deep-Sea Res. I*, **54**, 1361–1389,
824 doi:10.1016/j.dsr.2007.04.010.
825 Ridgway, K. R., and J. R. Dunn, 2007: Observational evidence for a Southern
826 Hemisphere oceanic supergyre. *Geophys. Res. Lett.*, **34**, L13612,
827 doi:10.1029/2007GL030392.
828 Rojas, M. and Coauthors, 2008: The Southern Westerlies during the last glacial
829 maximum in PMIP2 simulations. *Climate Dyn.*, **32**, 525–548,
830 doi:10.1007/s00382-008-0421-7.
831 Rouault, M., P. Penven, and B. Pohl, 2009: Warming in the Agulhas Current system
832 since the 1980's. *Geophys. Res. Lett.*, **36**, L12602, doi:10.1029/2009GL037987.
833 Shchepetkin, A. F., and J. C. McWilliams, 1998: Quasi-monotone advection schemes
834 based on explicit locally adaptive dissipation. *Mon. Wea. Rev.*, **126**, 1542–1580.

835 Shchepetkin, A. F., and J. C. McWilliams, 2005: The regional oceanic modeling system
836 (ROMS): a split-explicit, free-surface, topography-following-coordinate oceanic
837 model. *Ocean Modell.*, **9**, 347–404, doi:10.1016/j.ocemod.2004.08.002.
838 Sijp, W. P., and M. H. England, 2008: The effect of a northward shift in the southern
839 hemisphere westerlies on the global ocean. *Prog. Oceanogr.*, **79**, 1–19,
840 doi:10.1016/j.pocean.2008.07.002.
841 Sijp, W. P., and M. H. England, 2009: Southern Hemisphere Westerly Wind Control over
842 the Ocean's Thermohaline Circulation. *J. Climate*, **22**, 1277–1286,
843 doi:10.1175/2008JCLI2310.1.
844 Smagorinsky, J., 1963: General circulation experiments with the primitive equations. I.
845 The basic experiment. *Mon. Wea. Rev.*, **27**, 99–164.
846 Son, S.-W. and Coauthors, 2010: Impact of stratospheric ozone on Southern Hemisphere
847 circulation change: A multimodel assessment. *J. Geophys. Res.*, **115**, D00M07,
848 doi:10.1029/2010JD014271.
849 Speich, S., B. Blanke, and G. Madec, 2001: Warm and cold water routes of an OGCM
850 thermohaline conveyor belt. *Geophys. Res. Lett.*, **28**, 311–314.
851 Spence, P., J. C. Fyfe, A. Montenegro, and A. J. Weaver, 2010: Southern Ocean
852 Response to Strengthening Winds in an Eddy-Permitting Global Climate Model.
853 *J. Climate*, **23**, 5332–5343, doi:10.1175/2010JCLI3098.1.
854 Steele, M., R. Morfley, and W. Ermold, 2001: PHC: A global ocean hydrography with
855 high-quality Artic Ocean. *J. Climate*, **14**, 2079–2087.

856 Swart, N. C., and J. C. Fyfe, 2012: Observed and simulated changes in the Southern
857 Hemisphere surface westerly wind-stress. *Geophys. Res. Lett.*, **39**, 6–11,
858 doi:10.1029/2012GL052810.
859 Taylor, K. E., R. J. Stouffer, and G. A. Meehl, 2012: An Overview of CMIP5 and the
860 Experiment Design. *Bull. Amer. Meteor. Soc.*, **93**, 485–498, doi:10.1175/BAMS-
861 D-11-00094.1.
862 The DRAKKAR Group, 2007: Eddy-permitting ocean circulation hindcasts of past
863 decades. *CLIVAR Exchanges*, Vol. 12 of, 8–14.
864 Toggweiler, J. R., J. L. Russell, and S. R. Carson, 2006: Midlatitude westerlies,
865 atmospheric CO 2 , and climate change during the ice ages. *Paleoceanography*,
866 **21**, 1–15, doi:10.1029/2005PA001154.
867 Tréguier A.-M., 1992: Kinetic energy analysis of an eddy resolving, primitive equation
868 North Atlantic model. *J. Geophys. Res.*, **97**, 687–701.
869 van Sebille, E., A. Biastoch, P. J. van Leeuwen, and W. P. M. de Ruijter, 2009: A weaker
870 Agulhas Current leads to more Agulhas leakage. *Geophys. Res. Lett.*, **36**, L03601,
871 doi:10.1029/2008GL036614.
872 van Sebille, E., and P. J. van Leeuwen, 2007: Fast northward energy transfer in the
873 Atlantic due to Agulhas rings. *J. Phys. Oceanogr.*, **37**, 2305–2315,
874 doi:10.1175/JPO3108.1.
875 van Sebille, E., P. J. van Leeuwen, A. Biastoch, and W. P. M. de Ruijter, 2010: Flux
876 comparison of Eulerian and Lagrangian estimates of Agulhas leakage: A case
877 study using a numerical model. *Deep-Sea Res. I*, **57**, 319–327,
878 doi:10.1016/j.dsr.2009.12.006.

879 Watson, P. a. G., D. J. Karoly, M. R. Allen, N. Faull, and D. S. Lee, 2012: Quantifying
880 uncertainty in future Southern Hemisphere circulation trends. *Geophys. Res. Lett.*,
881 **39**, L23708, doi:10.1029/2012GL054158.
882 Weijer, W. and Coauthors, 2012: The Southern Ocean and Its Climate in CCSM4. *J.*
883 *Climate*, **25**, 2652–2675, doi:10.1175/JCLI-D-11-00302.1.
884 Wyrwoll, K.-H., B. Dong, and P. Valdes, 2000: On the position of southern hemisphere
885 westerlies at the Last Glacial Maximum: an outline of AGCM simulation results
886 and evaluation of their implications. *Quat. Sci. Rev.*, **19**, 881–898,
887 doi:10.1016/S0277-3791(99)00047-5.
888 Zahn, R., J. R. E. Lutjeharms, A. Biastoch, G. Knorr, W. Park, C. J. C. Reason, 2010:
889 Investigating the Global Impacts of the Agulhas Current. *Eos. Trans. AGU,* **91**,
890 109-110.
891 Zalesak, S. T., 1979: Fully multidimensional flux corrected transport algorithms for
892 fluids. *J. Comput. Phys.*, **31**, 335–362.
893
894

List of Figures

FIG. 1. Mid-depth (250 – 400m) temperature (shading, °C) and velocity gradients (shown as the 3-dimentional-depth expression), 5-day average snapshot centered at 17 Jun 2006 from the hind-cast realization of INALT01 illustrating the major pathway of Agulhas leakage across the South Atlantic. The INALT01 configuration consists of a global half-degree model with a tenth-degree nest over the region demarked by the grey box (50°S – 8°N, 70°W – 70°E).

FIG. 2. Volume integrated (10°W – 60°E; 10° – 45°S) kinetic energy per unit mass ($m^2\ s^{-2}$) with annual values (thick lines) overlaying monthly values (grey). Following a 20 year spin-up, reference (REF, black lines) experiments were performed for all three models. Wind anomalies were added from year 31; example of the SHW+40% (red lines) runs is shown. For the purpose of clarity, INALT01 values are offset by $1 \times 10^{20}\ m^2\ s^{-2}$. Common analysis period (model years 51 – 60) for Fig. 6 is indicated by the blue shading.

FIG. 3. (a) Wind stress magnitude (shading, $N\ m^{-2}$) and direction (vector) with horizontal barotropic stream-function contours overlay (data extracted from ORCA05-REF experiment); contour interval at 10 and 25 Sv for negative (dashed line) and positive (full lines) values respectively, thick contour represent the zero-line. (b) and (c) Zonally averaged (20° – 115°E) wind-stress ($N\ m^{-2}$) with thick black curve indicating the time-reference case. (b) Westerly position altered by -4° (blue), -2° (green), +2° (pink) and +4° (red) about the mean (black), without changing the total energy input. (c) Intensity

change by -40 % (blue), -20 % (green), +20 % (pink), and +40 % (red) of the mean (black). Wind changes are applied within the region 35° – 63°S.

FIG. 4. Application of the SHW+40% anomaly (40 % intensification of westerlies). The wind stress anomaly (N m^{-2}) is applied (a) circumpolarly (FULL); (b) circumpolarly except the region bounded by 0° – 35°E, north of 45°S (BASIN); (c) only over the region bounded by 0° – 35°E, north of 45°S (LOCAL); (d) over region west of 18°E and east of 115°E (ACC-P); (e) between region 18°W – 115°E (ACC-B); and (f) between region 0° – 35°E (ACC-L).

FIG. 5. Representation of mean circulation (contours of sea surface height (SSH) averaged for period 1992 – 2007) and mesoscale variability (shading of SSH variance, cm^2) from (a) altimetric observation AVISO, (b) ORCA05, (c) AGIO and (d) INALT01. Sections used to measure Agulhas leakage across the Good-Hope Line (GH), the Agulhas Current (AC), the Mozambique throughflow (Moz) and the region where the Agulhas Return Current is monitored (box) are shown in (b). The domain used for the Lagrangian analysis is shown in (d).

FIG. 6. Change in Agulhas leakage (%) versus change in (a) position (°Lat) and (b & c) intensity (%) of the Southern Hemisphere westerlies (SHW). Reference values (black dot) are set at the origin for all three models and each dot represents a decade average (model years 51 – 60, blue shading in Fig. 2). (c) The decomposition between FULL,

940 BASIN and LOCAL is shown for the SHW-40% and SHW+40% cases. The gray line in
941 b & c represent the theoretical change in Sverdrup transport.
942
943 FIG. 7. Time-series for the REF and SHW+40% cases within ORCA05. Sections used to
944 measure the transports are shown in Fig. 5a and aside from the Agulhas leakage (AL), all
945 transports are measured from the barotropic stream-function: the Antarctic Circumpolar
946 Current (ACC) as the maximum stream-function south of Africa between 20° and 30°E;
947 the sub-gyre strength as the minimum stream-function value between 30° and 60°E; the
948 Agulhas Current (AC) as the minimum stream-function along the section at 32°S. For the
949 Agulhas Return Current (ARC), speed is for the top 1000 m. The light red, yellow and
950 blue shadings indicate Stage-1, Stage-2 and Stage-3 in ORCA05-SHW+40%-FULL
951 leakage response respectively (details in text).
952
953 FIG. 8. Same as Fig. 7 for INALT01.
954
955 FIG. 9. Time-series of Agulhas leakage (AL), Agulhas Return Current variance (ARC
956 Var) and Antarctic Circumpolar Current (ACC) transport from the ACC-P (pink), ACC-B
957 (blue) and ACC-L (green) decompositions of the SHW+40% anomaly within ORCA05.
958 The light red, yellow and blue shadings indicate Stage-1, Stage-2 and Stage-3 in
959 ORCA05-SHW+40%-FULL leakage response respectively (extracted from Fig. 7).
960
961 FIG. 10. Eddy Kinetic Energy (EKE) per unit mass anomaly at 100 m ($cm^2\ s^{-2}$) within
962 ORCA05 (left) and INALT01 (right) averaged over model years 41 – 45 (a & c) and 56 –

963 60 (b & d). Contours indicate the respective averaged reference EKE values for model
964 years 41 - 60.
965
966 FIG. 11. Schematic of the proposed mechanism of leakage response to the westerlies.
967 Contours of barotropic stream function portray the anticyclonic supergyre (shaded area)
968 connecting the South Indian and South Atlantic oceans, with thick black contour
969 demarcating its boundaries (data extracted from ORCA05-REF experiment). Thick
970 arrows indicate the meridional Sverdrup interior flow and the corresponding zonal
971 transport that results from the wind stress application (REF in black and SHW+40% case
972 in red). The circulation is closed by the return flow of the western boundary currents
973 (dotted arrows).
974
975 FIG. 12. Change in Agulhas leakage (%) versus change in wind stress (%) averaged over
976 the region 20°W – 140°E, 35° - 65°S. Squares represent decadal averages from hind-cast
977 inter-annual (IA) simulations of ORCA05-IA (light blue) and INALT01-IA (light green),
978 with the period 1964-1973 taken as reference (set at origin); Circles represent Stage-1
979 averages (model years 41-45) from the FULL application of the SHW+20% and
980 SHW+40% anomalies as well as the corresponding REF (set at origin) within ORCA05
981 (blue) and INALT01 (green).

982 TABLE 1. Sensitivity experiments and their integration periods (in years). IA: Inter-
983 Annual; REF: Reference; SHW: Southern Hemisphere westerlies. Domain
984 decompositions are depicted in Fig. 4.

Experiment	Domain	Description	Model Configurations		
			ORCA05	AGIO	INALT01
IA	n/a	Inter-annual Reference	1948 – 2007		1948 – 2007
REF	n/a	Climatological Reference	1 – 110	1 – 60	1 – 60
SHW+4	FULL	4º Equatorward shift	31 – 60		31 – 60
SHW+2	FULL	2º Equatorward shift	31 – 60		
SHW-2	FULL	2º Poleward shift	31 – 60		31 – 60
SHW-4	FULL	4º Poleward shift	31 – 60		
SHW-40%	FULL	40 % Intensity decrease	31 – 110	31 – 60	31 – 60
	BASIN		31 – 60		
	LOCAL		31 – 60		
SHW-20%	FULL	20 % Intensity decrease	31 – 60	31 – 60	
SHW+20%	FULL	20 % Intensity increase	31 – 60	31 – 60	
SHW+40%	FULL	40 % Intensity increase	31 – 110	31 – 60	31 – 60
	BASIN		31 – 80		
	LOCAL		31 – 80		31 – 60
	ACC-P		31 – 60		
	ACC-B		31 – 60		
	ACC-L		31 – 60		
	ACC	AGIO boundary condition*	n/a	31 – 60	n/a

985 *Further details in text.
986

987

988

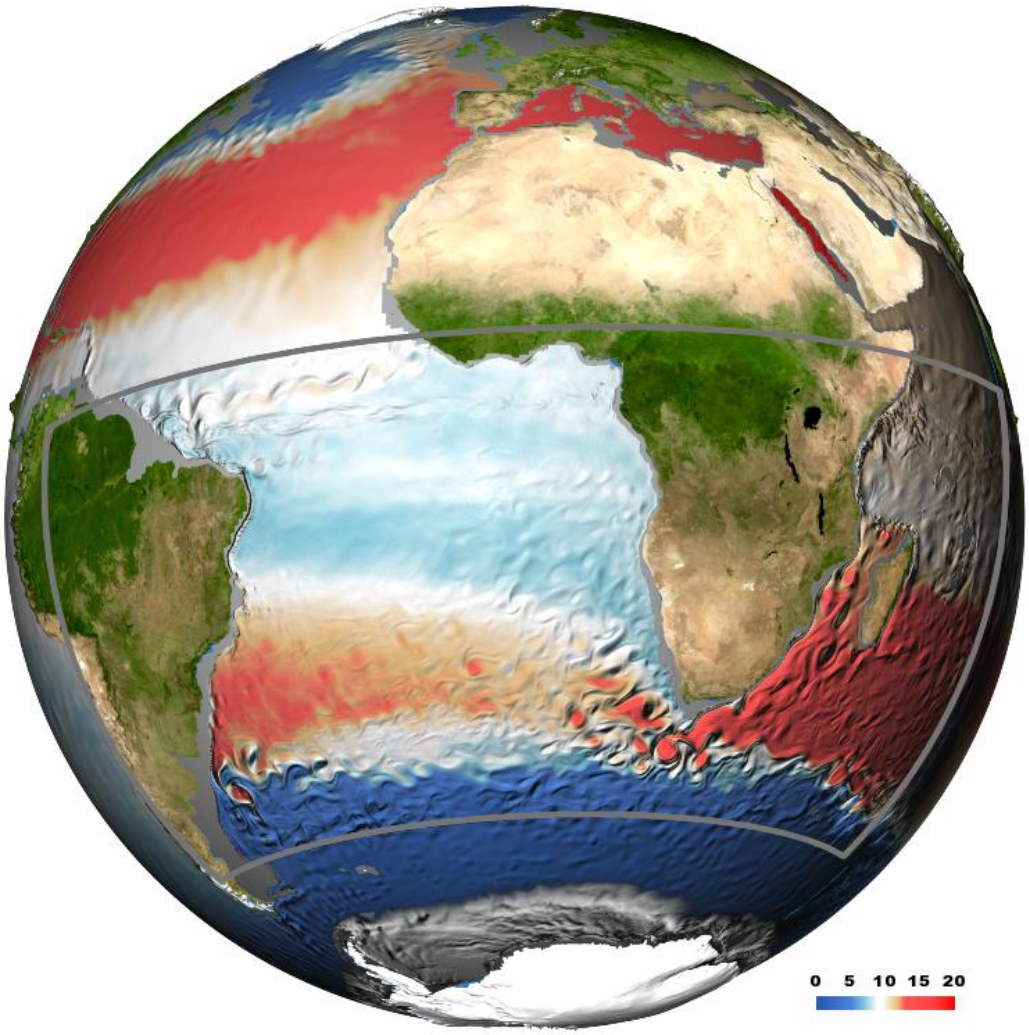

989

990 FIG. 1. Mid-depth (250 – 400m) temperature (shading, °C) and velocity gradients (shown
991 as the 3-dimentional-depth expression), 5-day average snapshot centered at 17 Jun 2006
992 from the hind-cast realization of INALT01 illustrating the major pathway of Agulhas
993 leakage across the South Atlantic. The INALT01 configuration consists of a global half-
994 degree model with a tenth-degree nest over the region demarked by the grey box (50°S –
995 8°N, 70°W – 70°E).

996

997

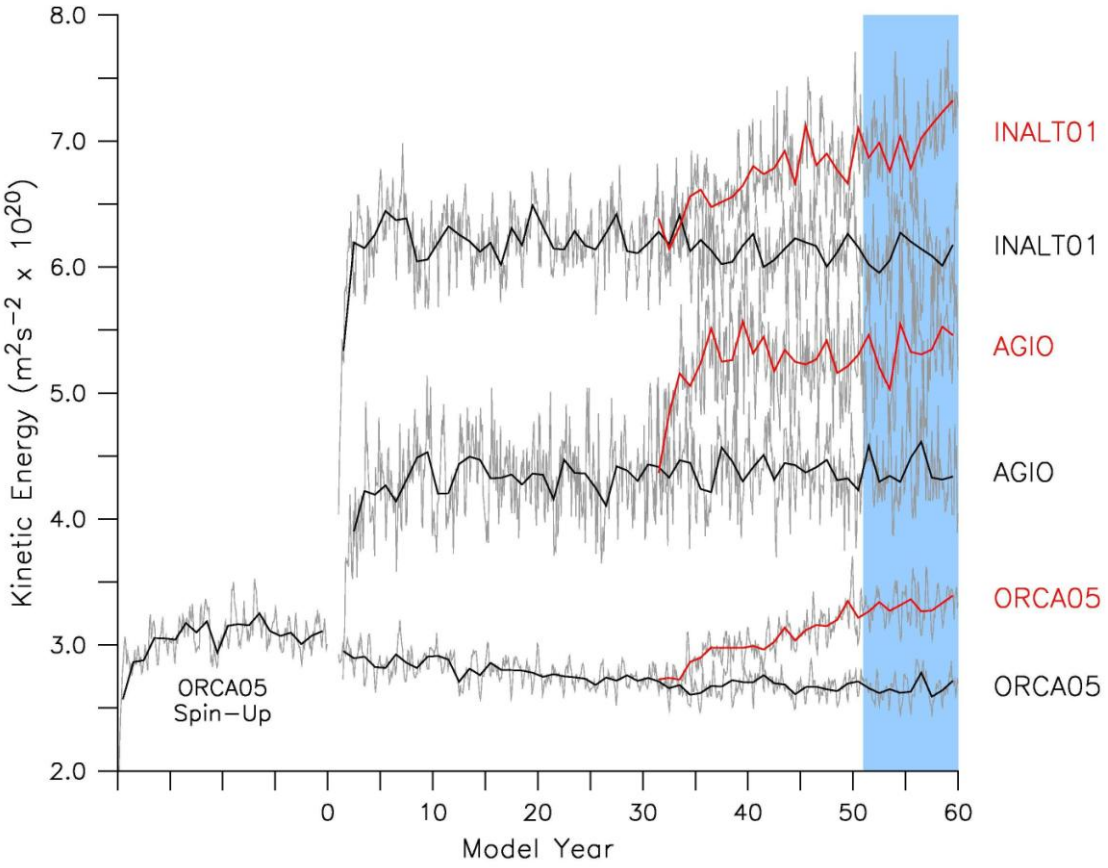

998

999 FIG. 2. Volume integrated (10°W – 60°E; 10° – 45°S) kinetic energy per unit mass (m^2 s^{-2})
1000 with annual values (thick lines) overlaying monthly values (grey). Following a 20 year
1001 spin-up, reference (REF, black lines) experiments were performed for all three models.
1002 Wind anomalies were added from year 31; example of the SHW+40% (red lines) runs is
1003 shown. For the purpose of clarity, INALT01 values are offset by 1 x 10^{20} m^2 s^{-2}.
1004 Common analysis period (model years 51 – 60) for Fig. 6 is indicated by the blue
1005 shading.

1006

1007

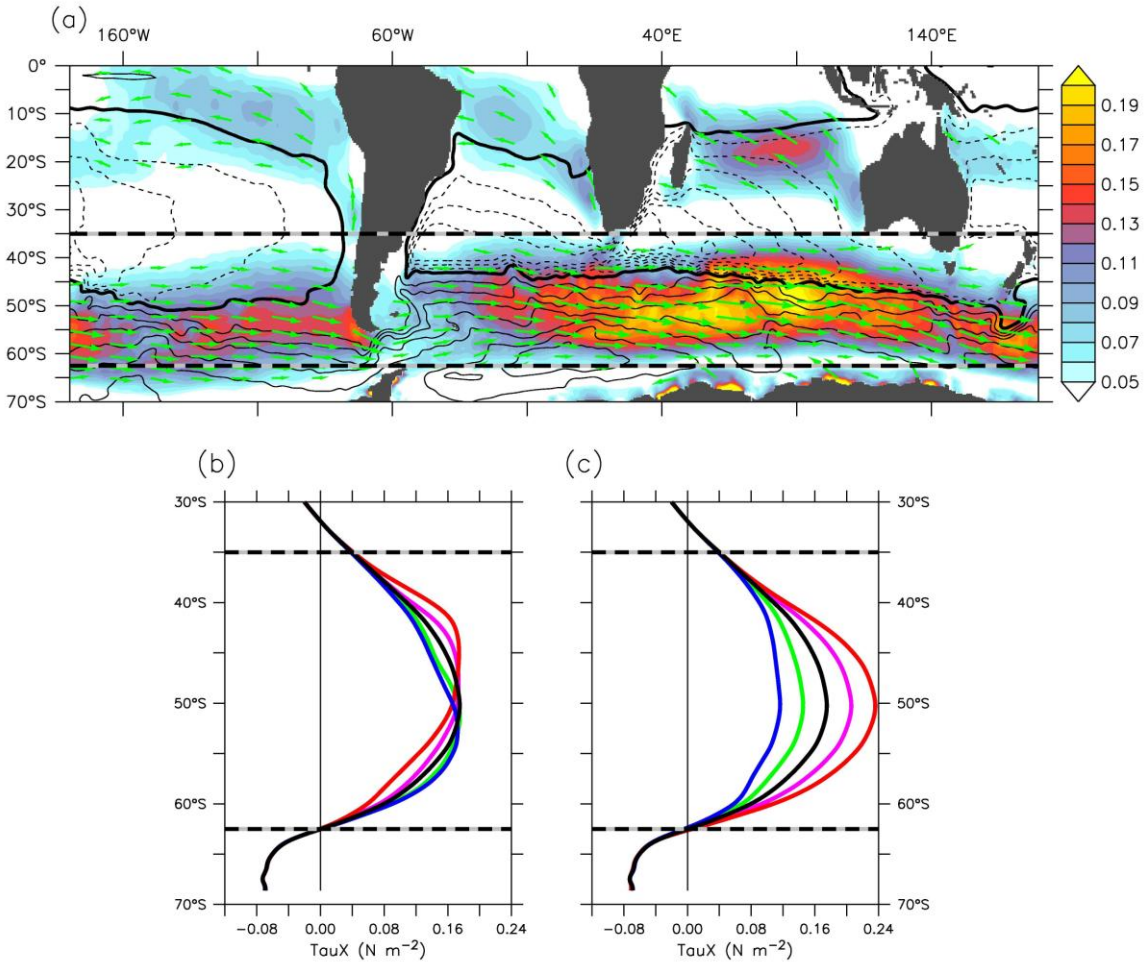

1008

1009 FIG. 3. (a) Wind stress magnitude (shading, N m^{-2}) and direction (vector) with horizontal
1010 barotropic stream-function contours overlay (data extracted from ORCA05-REF
1011 experiment); contour interval at 10 and 25 Sv for negative (dashed line) and positive (full
1012 lines) values respectively, thick contour represent the zero-line. (b) and (c) Zonally
1013 averaged (20° – 115°E) wind-stress (N m^{-2}) with thick black curve indicating the time-
1014 reference case. (b) Westerly position altered by -4° (blue), -2° (green), +2° (pink) and +4°
1015 (red) about the mean (black), without changing the total energy input. (c) Intensity
1016 change by -40 % (blue), -20 % (green), +20 % (pink), and +40 % (red) of the mean
1017 (black). Wind changes are applied within the region 35° – 63°S.

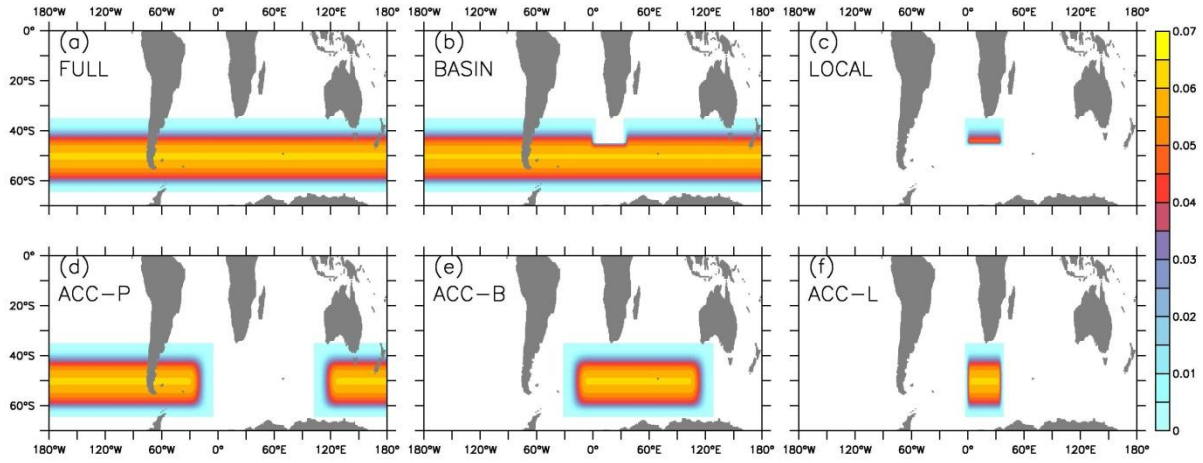

FIG. 4. Application of the SHW+40% anomaly (40 % intensification of westerlies). The wind stress anomaly (N m^{-2}) is applied (a) circumpolarly (FULL); (b) circumpolarly except the region bounded by 0° – 35°E, north of 45°S (BASIN); (c) only over the region bounded by 0° – 35°E, north of 45°S (LOCAL); (d) over region west of 18°E and east of 115°E (ACC-P); (e) between region 18°W – 115°E (ACC-B); and (f) between region 0° – 35°E (ACC-L).

1029

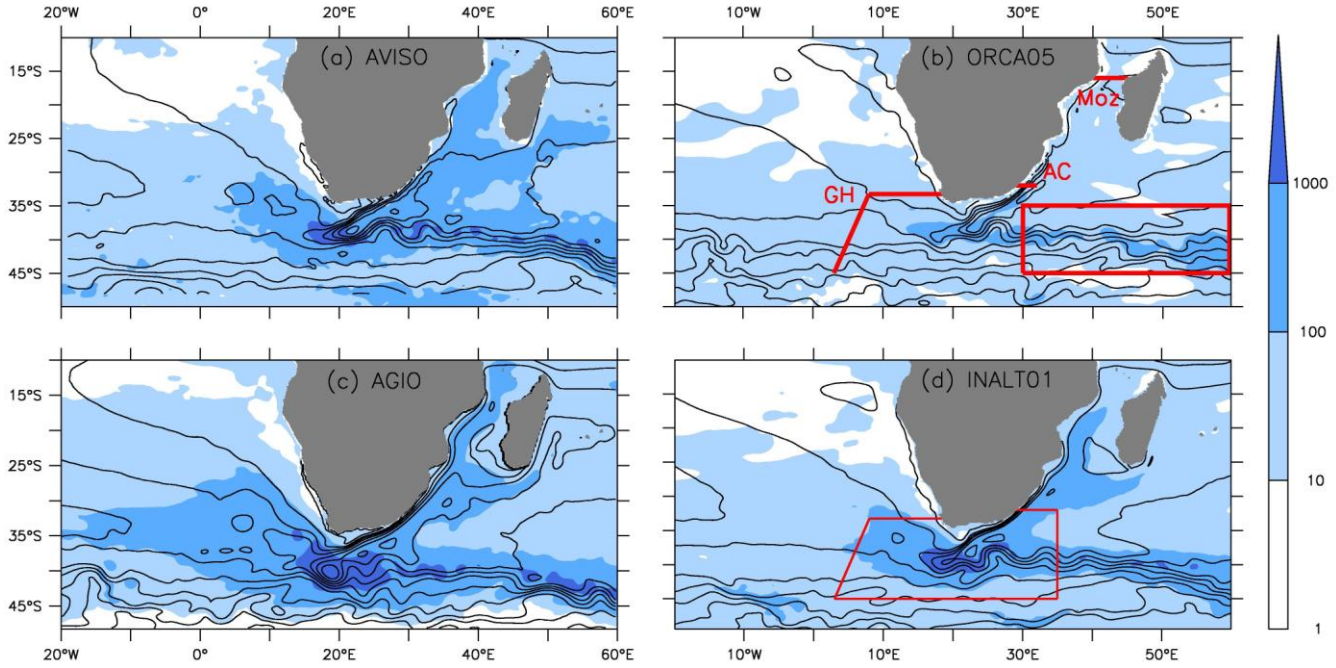

1030

1031 FIG. 5. Representation of mean circulation (contours of sea surface height (SSH)

1032 averaged for period 1992 – 2007) and mesoscale variability (shading of SSH variance,

1033 cm^2) from (a) altimetric observation AVISO, (b) ORCA05, (c) AGIO and (d) INALT01.

1034 Sections used to measure Agulhas leakage across the Good-Hope Line (GH), the Agulhas

1035 Current (AC), the Mozambique throughflow (Moz) and the region where the Agulhas

1036 Return Current is monitored (box) are shown in (b). The domain used for the Lagrangian

1037 analysis is shown in (d).

1038

1039

1040

(a) SHW - Position

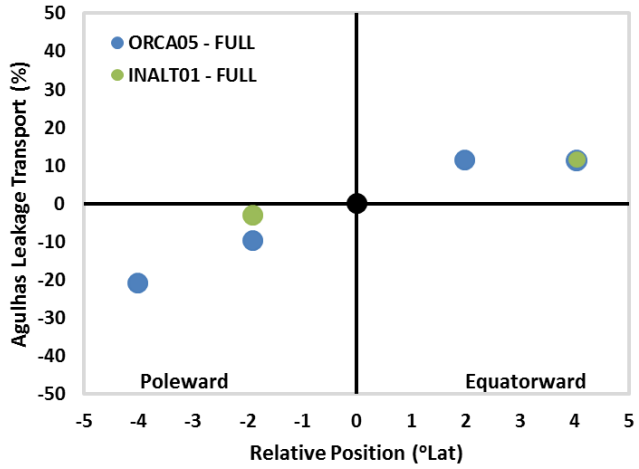

(b) SHW - Intensity

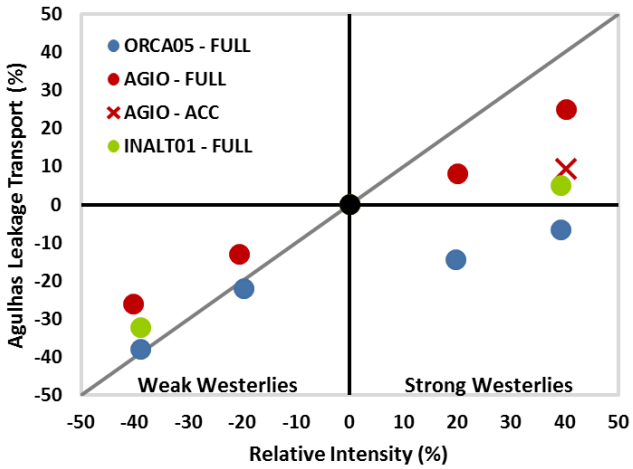

(c) SHW - Intensity Decomposition

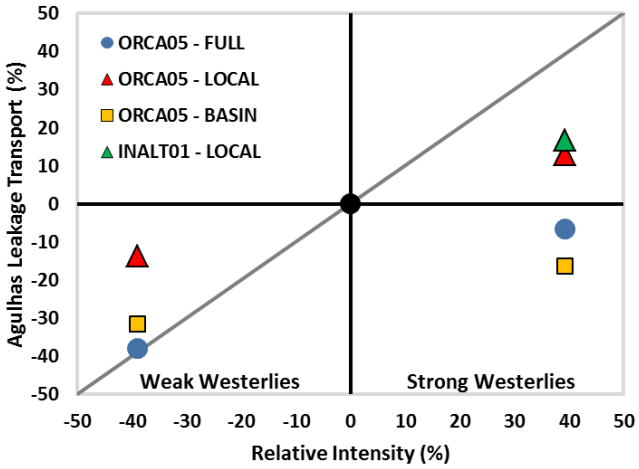

1041

1042 FIG. 6. Change in Agulhas leakage (%) versus change in (a) position (°Lat) and (b & c)
1043 intensity (%) of the Southern Hemisphere westerlies (SHW). Reference values (black
1044 dot) are set at the origin for all three models and each dot represents a decade average
1045 (model years 51 – 60, blue shading in Fig. 2). (c) The decomposition between FULL,
1046 BASIN and LOCAL is shown for the SHW-40% and SHW+40% cases. The gray line in
1047 b & c represent the theoretical change in Sverdrup transport.
1048
1049

1050

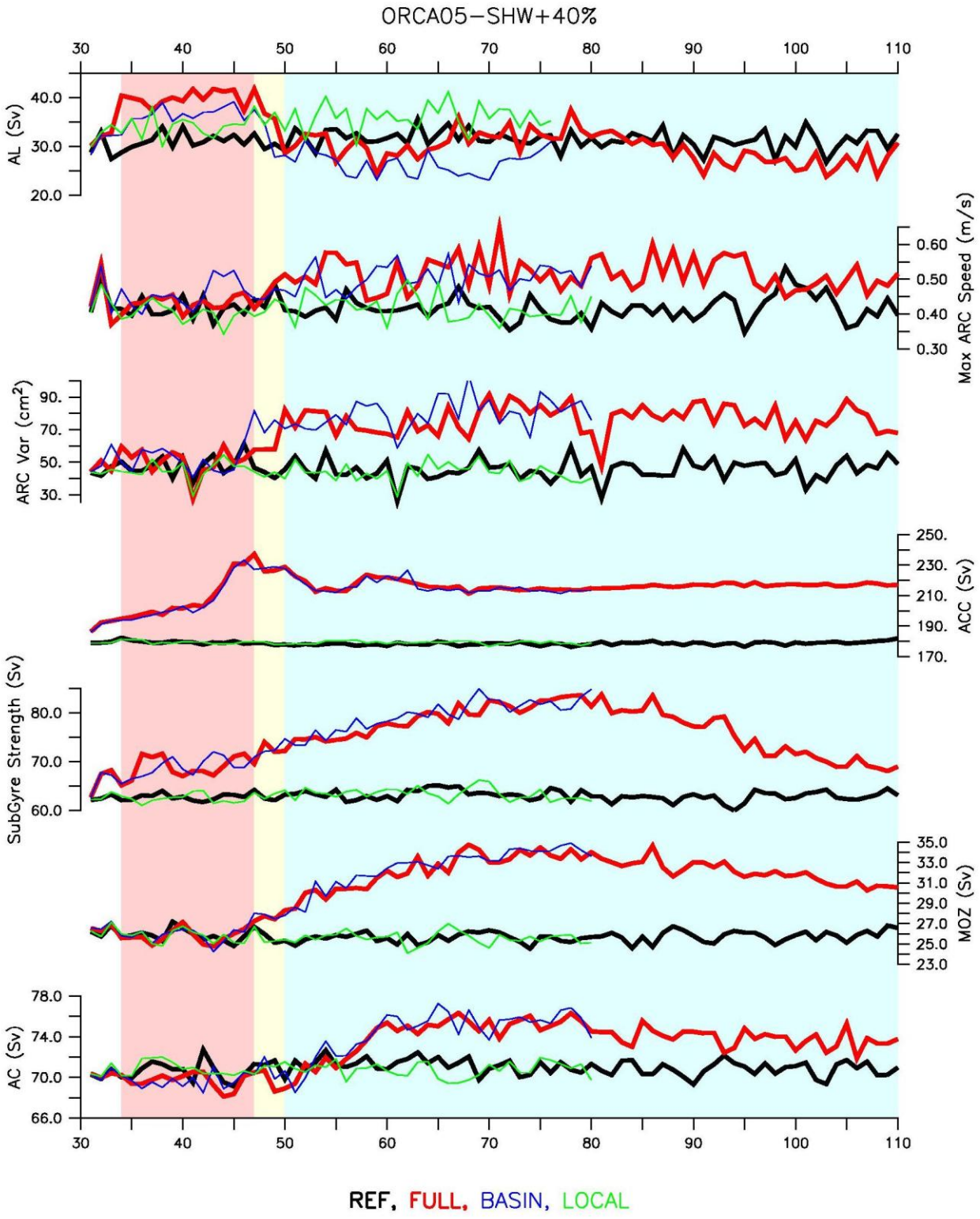
ORCA05−SHW+40%
AL (Sv)
Max ARC Speed (m/s)
ARC Var (cm²)
ACC (Sv)
SubGyre Strength (Sv)
MOZ (Sv)
AC (Sv)
REF, FULL, BASIN, LOCAL

1051

1052 FIG. 7. Time-series for the REF and SHW+40% cases within ORCA05. Sections used to
1053 measure the transports are shown in Fig. 5a and aside from the Agulhas leakage (AL), all
1054 transports are measured from the barotropic stream-function: the Antarctic Circumpolar
1055 Current (ACC) as the maximum stream-function south of Africa between 20° and 30°E;
1056 the sub-gyre strength as the minimum stream-function value between 30° and 60°E; the
1057 Agulhas Current (AC) as the minimum stream-function along the section at 32°S. For the
1058 Agulhas Return Current (ARC), speed is for the top 1000 m. The light red, yellow and
1059 blue shadings indicate Stage-1, Stage-2 and Stage-3 in ORCA05-SHW+40%-FULL
1060 leakage response respectively (details in text).
1061

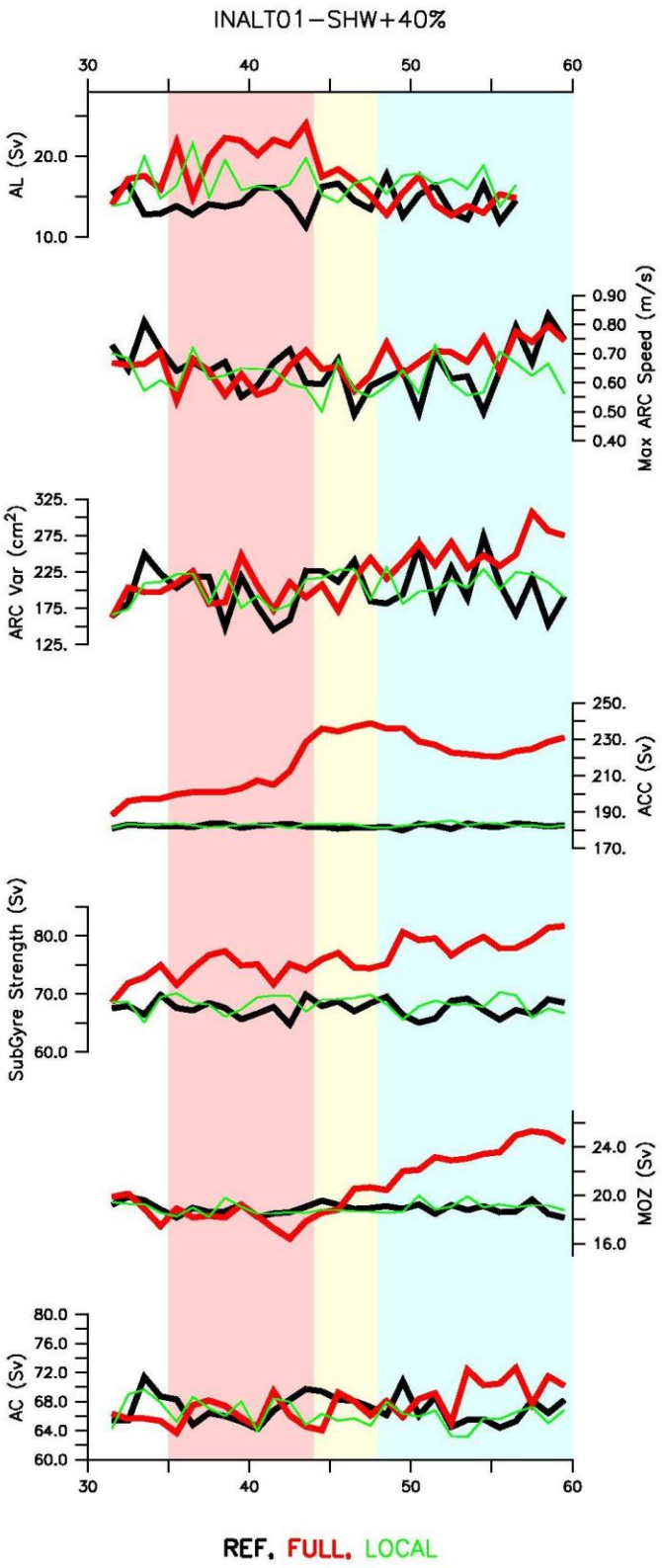

1062

1063 FIG. 8. Same as Fig. 7 for INALT01.

1064

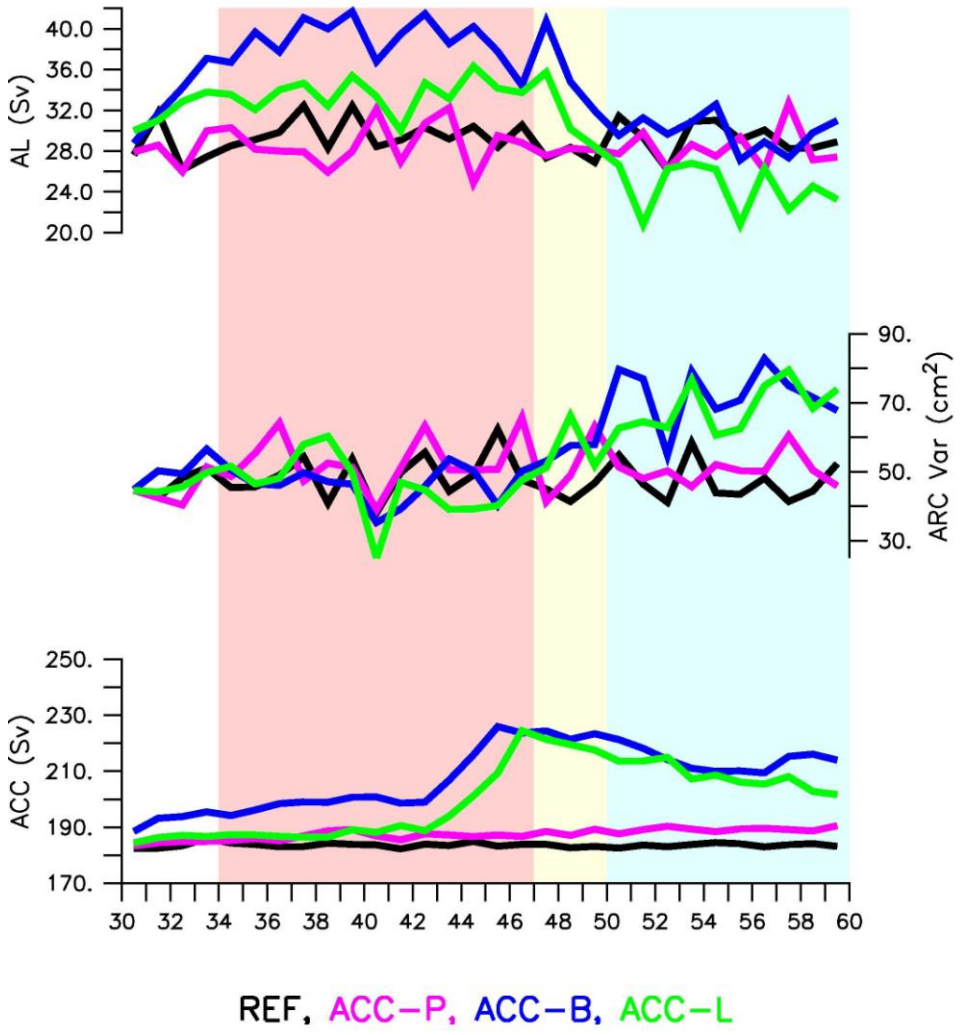

1065

1066 FIG. 9. Time-series of Agulhas leakage (AL), Agulhas Return Current variance (ARC
1067 Var) and Antarctic Circumpolar Current (ACC) transport from the ACC-P (pink), ACC-B
1068 (blue) and ACC-L (green) decompositions of the SHW+40% anomaly within ORCA05.
1069 The light red, yellow and blue shadings indicate Stage-1, Stage-2 and Stage-3 in
1070 ORCA05-SHW+40%-FULL leakage response respectively (extracted from Fig. 7).

1071

1072

1073

1074

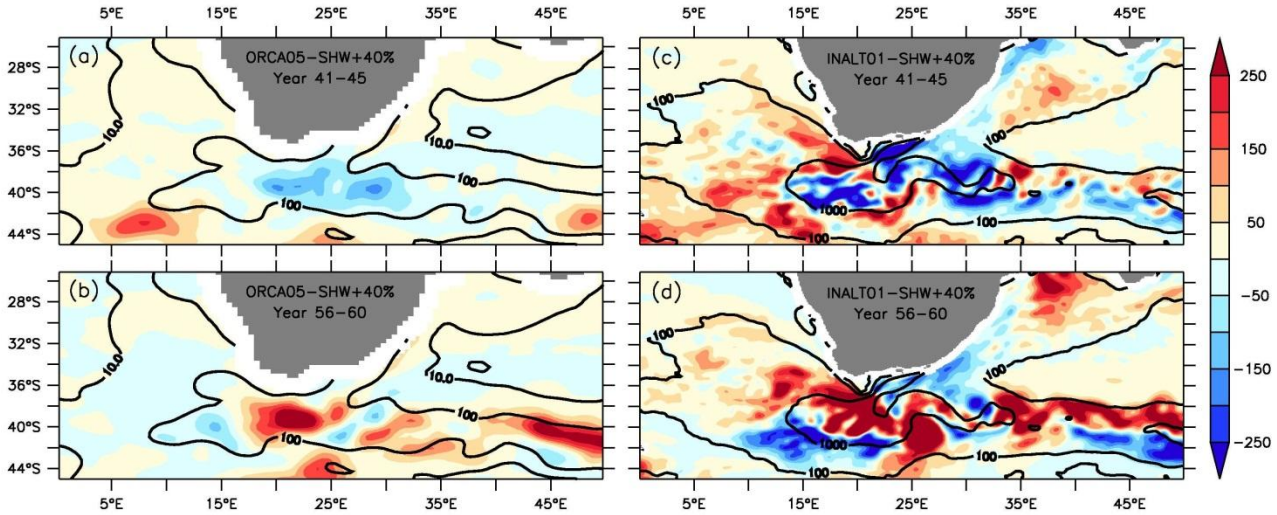

1075

1076 FIG. 10. Eddy Kinetic Energy (EKE) per unit mass anomaly at 100 m (cm^2 s^{-2}) within

1077 ORCA05 (left) and INALT01 (right) averaged over model years 41 – 45 (a & c) and 56 –

1078 60 (b & d). Contours indicate the respective averaged reference EKE values for model

1079 years 41 - 60.

1080

1081

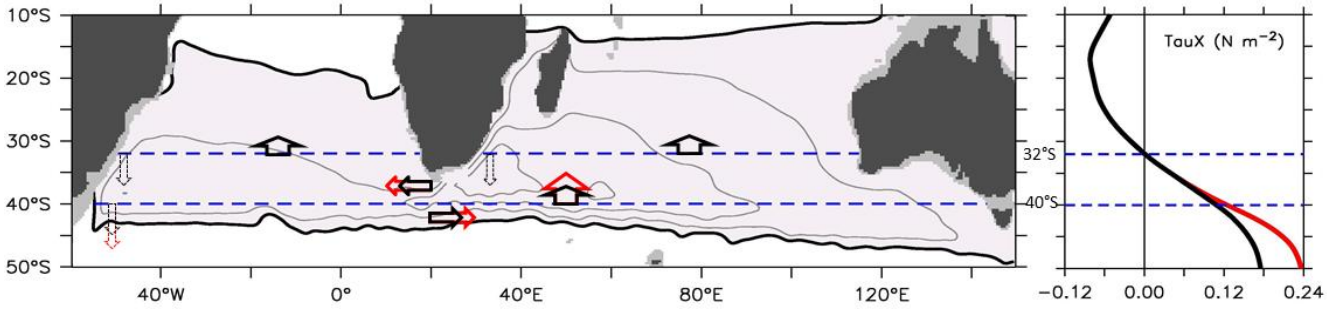

1082

1083 FIG. 11. Schematic of the proposed mechanism of leakage response to the westerlies.

1084 Contours of barotropic stream function portray the anticyclonic supergyre (shaded area)

1085 connecting the South Indian and South Atlantic oceans, with thick black contour

1086 demarcating its boundaries (data extracted from ORCA05-REF experiment). Thick

1087 arrows indicate the meridional Sverdrup interior flow and the corresponding zonal

1088 transport that results from the wind stress application (REF in black and SHW+40% case

1089 in red). The circulation is closed by the return flow of the western boundary currents

1090 (dotted arrows).

1091

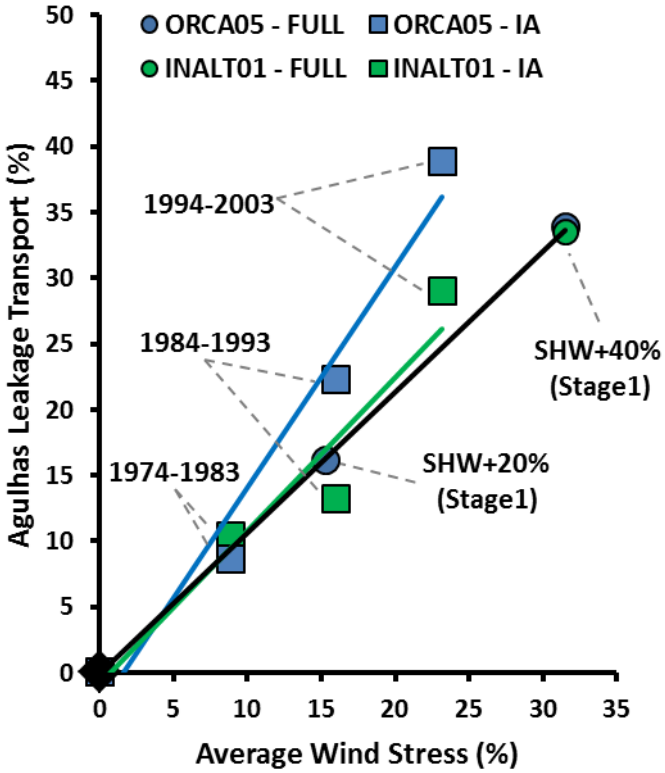

1092

1093 FIG. 12. Change in Agulhas leakage (%) versus change in wind stress (%) averaged over
1094 the region 20°W – 140°E, 35° - 65°S. Squares represent decadal averages from hind-cast
1095 inter-annual (IA) simulations of ORCA05-IA (light blue) and INALT01-IA (light green),
1096 with the period 1964-1973 taken as reference (set at origin); Circles represent Stage-1
1097 averages (model years 41-45) from the FULL application of the SHW+20% and
1098 SHW+40% anomalies as well as the corresponding REF (set at origin) within ORCA05
1099 (blue) and INALT01 (green).

1100